

Supplementary Appendix

This appendix has been provided by the authors to give readers additional information about their work.

Supplement to: Roberts KG, Li Y, Payne-Turner D, et al. Targetable kinase-activating lesions in Ph-like acute lymphoblastic leukemia. *N Engl J Med* 2014;371:1005-15. DOI: [10.1056/NEJMoa1403088](https://doi.org/10.1056/NEJMoa1403088)

SUPPLEMENTARY APPENDIX

for

Targetable kinase activating lesions in Ph-like acute lymphoblastic leukemia

Kathryn G. Roberts^{1*}, Ph.D., Yongjin Li^{2,7*}, Ph.D., Debbie Payne-Turner¹, B.S., Richard C. Harvey^{3,39}, Ph.D., Yung-Li Yang¹, M.D., Deqing Pei⁴, M.S., Kelly McCastlain¹, B.S., Li Ding^{5,6,7}, Ph.D., Charles Lu^{5,6,7}, Ph.D., Guangchun Song¹, M.S., Jing Ma¹, Ph.D., Jared Becksfort², M.S., Michael Rusch^{2,7}, B.A., Shann-Ching Chen¹, Ph.D., John Easton⁷, Ph.D., Jinjun Cheng^{1,7}, M.D., Kristy Boggs⁷, Ph.D., Natalia Santiago-Morales¹, B.S., Ilaria Iacobucci¹, Ph.D., Robert S. Fulton^{5,6,7}, Ph.D., Ji Wen¹, Ph.D., Marcus Valentine⁸, B.A., Cheng Cheng⁴, Ph.D., Steven W. Paugh⁹, Ph.D., Meenakshi Devidas^{10,37}, Ph.D., I-Ming Chen^{3,37}, D.V.M., Shalini Reshmi^{11,37}, Ph.D., Amy Smith¹¹, B.S., Erin Hedlund^{2,7}, Ph.D., Pankaj Gupta^{2,7}, M.S., Panduka Nagahawatte^{2,7}, M.S., Gang Wu^{2,7}, Ph.D., Xiang Chen^{2,7}, Ph.D., Donald Yergeau⁷, Ph.D., Bhavin Vadodaria⁷, B.A., Heather Mulder⁷, B.S., Naomi J. Winick¹², M.D., Eric C. Larsen¹³, M.D., William L. Carroll^{14,37}, M.D., Nyla A. Heerema¹⁵, Ph.D., Andrew J. Carroll¹⁶, Ph.D., Guy Grayson¹⁷, M.D., Sarah K. Tasian¹⁸, M.D., Andrew S. Moore¹⁹, M.D., Frank Keller²⁰, M.D., Melissa Frei-Jones²¹, M.D., James A. Whitlock²², M.D., Elizabeth A. Raetz²³, Deborah L. White²⁴, Ph.D., Timothy P. Hughes²⁴, M.D., Jaime M. Guidry Auvil^{25,37}, Ph.D., Malcolm A. Smith^{26,37}, M.D., Guido Marcucci²⁷, M.D., Clara D. Bloomfield²⁷, M.D., Krzysztof Mrózek²⁷, Ph.D., Jessica Kohlschmidt^{27,28}, Ph.D., Wendy Stock²⁹, M.D., Steven M. Kornblau³⁰, M.D., Marina Konopleva³⁰, M.D., Elisabeth Paietta³¹, Ph.D., Ching-Hon Pui³², M.D., Sima Jeha³², M.D., Mary V. Relling^{7,9,37}, Pharm.D., William E. Evans^{7,9}, Pharm.D., Daniela S. Gerhard^{25,37}, Ph.D., Julie M. Gastier-Foster^{11,37}, Ph.D., Elaine Mardis^{5,6,7,33}, Ph.D., Richard K. Wilson^{5,6,7,33}, Ph.D., Mignon L. Loh^{34,37}, M.D., James R. Downing^{1,7,35,37}, M.D., Stephen P. Hunger^{36,37}, M.D., Cheryl L. Willman^{3,37}, M.D., Jinghui Zhang^{2,7,37}, Ph.D., and Charles G. Mullighan^{1,7,37}, M.D.

TABLE OF CONTENTS

SUPPLEMENTARY METHODS	5
Patients and clinical treatment protocols.....	5
Microarray analysis.....	5
Genome sequencing	6
Digital gene expression profiling.....	6
Identification of sequence mutations.....	7
Fluorescence <i>in situ</i> hybridization (FISH)	8
<i>In vitro</i> assays	9
Protein expression.....	9
Xenograft models	10
SUPPLEMENTARY RESULTS	11
Genomic profiling of Ph-like ALL.....	11
Case descriptions for tyrosine kinase inhibitor treatment of Ph-like ALL	11
SUPPLEMENTARY FIGURES	16
Figure S1. CONSORT diagram of B-ALL cases included in the study	16
Figure S2. Detailed outcome analyses of childhood, adolescent and young adult ALL	17
Figure S3. Janus kinase mutations.....	18
Figure S4. Microarray gene expression profiling.....	19
Figure S5. Principal components analysis of mRNA-seq data	20
Figure S6. Recurring kinase, B-cell pathway and tumor suppressor pathway alterations in Ph-like ALL	21
Figure S7. Frequency of Ph-like ALL subtypes in childhood high-risk (HR), adolescents and young adults.....	23
Figure S8. Kinase fusions in Ph-like ALL	24
Figure S9. Fluorescence <i>in situ</i> hybridization (FISH) of kinase fusions.....	29
Figure S10. CIRCOS plots.....	30

Figure S11. Ras pathway mutations	37
Figure S12. Subclonal mutations in Ph-like ALL	38
Figure S13. Clustering of Ph-like ALL subgroups	39
Figure S14. Outcome analyses between different subgroups in Ph-like ALL	40
Figure S15 Outcome analyses for <i>IKZF1</i> alteration	41
Figure S16. Experimental modeling of kinase fusions in Ph-like ALL.....	42
Figure S17. Treatment of Ph-like ALL xenografts with tyrosine kinase inhibitors	43
Figure S18. Flow chart for identification of Ph-like ALL cases and actionable kinase alterations	44
Figure S19. Sequence mutation analysis of Ph-like ALL.....	45
Figure S20. Non-kinase fusions.....	47
Figure S21. Genes involved in multiple rearrangements.....	50
SUPPLEMENTARY TABLES.....	51
Table S1. Patient cohort	51
Table S2. Clinical features and availability of genomic data.....	52
Table S3. B-ALL cases subjected to mRNA-sequencing	53
Table S4. Frequency of ALL subtypes in the study cohort	53
Table S5. Clinical characteristics and B-ALL subtype	54
Table S6. Minimal residual disease (MRD) analyses.....	55
Table S7. Multivariate analysis for childhood, adolescent and young adult B-ALL	56
Table S8. Sequencing coverage metrics	57
Table S9. Summary of genetic alterations in Ph-like ALL.....	57
Table S10. Gene expression profile of BCR-ABL1 and Ph-like ALL defined by mRNA-sequencing	57
Table S11. Fusions detected by next-generation sequencing.....	57
Table 12. Details of kinase fusions	57
Table S13. Summary of 5' and 3' fusion partner genes with multiple rearrangements	58

Table S14. Subclonal mutation analysis in Ph-like ALL	59
Table S15. Outcome analyses for different subgroups in Ph-like ALL.....	61
Table S16. Key genetic alterations in B-ALL.....	62
Table S17. B-ALL cases tested prospectively for Ph-like status.....	63
Table S18. Primer sequences for fusion verification, cloning and genomic PCR	66
Table S19. Probes used for fluorescence <i>in situ</i> hybridization	66
Table S20. Summary of sequence mutations in Ph-like ALL.....	67
Table S21. Summary of non-kinase fusions and association with kinase alterations.	67
SUPPLEMENTARY REFERENCES.....	68

SUPPLEMENTARY METHODS

Patients and clinical treatment protocols

Patients were obtained from the St Jude Children's Research Hospital Total XV¹; ClinicalTrials.gov Identifier NCT00137111) and Total XVI protocols (ClinicalTrials.gov Identifier NCT00549848); the COG P9906 high-risk B-ALL study²; the COG AALL0232 high-risk ALL study (ClinicalTrials.gov Identifier NCT00075725); the Eastern Cooperative Oncology Group E2993 trial³ (ClinicalTrials.gov Identifier NCT00002514); the MD Anderson Cancer Centre protocols⁴⁻⁷, and the Alliance – Cancer and Leukemia Group B protocols C19802 (ClinicalTrials.gov Identifier NCT00003700),⁸ C10102 (ClinicalTrials.gov Identifier NCT00061945) and C10403 (ClinicalTrials.gov Identifier NCT00558519). An overview of cases included from each protocol is provided in Figure S1. *BCR-ABL1* patients treated with the tyrosine kinase inhibitors imatinib or dasatinib are listed in Table S1. Treatment in Total XV and Total XVI trials was risk-stratified by minimal residual disease levels. All cases with available material were tested for chromosomal aneuploidies including hypodiploidy and hyperdiploidy, and known chromosomal rearrangements including *ETV6-RUNX1*, *TCF3-PBX1*, *BCR-ABL1* and rearrangements of *MLL* and *CRLF2*.

Microarray analysis

Gene expression profiling was performed for all samples using U133A or U133 Plus 2.0 microarrays as previously described (Affymetrix, Santa Clara, CA).⁹⁻¹¹ There were few significant differences in the clinical and laboratory features of patients with and without gene expression profiling data (Table S2). Ph-like ALL cases were identified using Predictive Analysis of Microarrays (PAM)¹² as previously described,¹¹ in which *BCR-ABL1*-positive cases in each cohort were used to identify a *BCR-ABL1* gene signature, and cases with a coefficient greater than 0.5 were deemed to be Ph-like. For clustering analysis, CEL files were normalized using default settings with the RMA algorithm in Expression Console (Affymetrix, build 1.3.1.187).

Affymetrix controls, globin and sex-associated probe sets (n=171) were removed and 340 ROSE outlier probe sets were selected from the remaining 54,504 probe sets based upon the presence of a group of at least 5% of the samples with a median intensity 5-fold higher or lower than predicted by trendlines¹³. Unsupervised hierarchical clustering was performed using MATLAB (MathWorks, version R2013b) using settings of Euclidean distance, standardization by row and complete linkage. DNA copy number alterations were determined using single nucleotide polymorphism (SNP) 500K and/or 6.0 microarrays (Affymetrix) and data analyzed using reference normalization and circular binary segmentation.¹⁴⁻¹⁶ For clustering of Ph-like samples, the top 5% most variable probesets from RMA scores were used.

Genome sequencing

Library construction was performed using Truseq exome capture baits and RNA-sequencing library preparation kits (Illumina), and sequencing performed on the HiSeq 2000.^{10,17} mRNA-seq data were mapped using StrongArm and rearrangements were identified using CICERO, a novel algorithm that assembles reads around breakpoints and maps the contig to the genome to find fusion transcripts (manuscripts in preparation). Putative fusions were validated by reverse transcription and polymerase chain reaction using Phusion (New England Biosciences) and Sanger or MiSeq (Illumina) sequencing. Primers are listed in Table S18.

Digital gene expression profiling

Transcript expression levels were estimated as Fragments Per Kilobase of transcript per Million mapped reads (FPKM) and gene FPKMs were computed by summing the transcript FPKMs for each gene using the Cuffdiff2 program.¹⁸ We called a gene “expressed” in a given sample if it had a FPKM value ≥ 0.35 based on the distribution of FPKM gene expression levels and excluded genes that were not expressed in any sample from the final gene expression data matrix for downstream analysis.

Clustering analysis was performed using junction reads from RNA-seq data. After \log_2 transformation, quantile normalization was used to adjust for different sequencing depths. Unsupervised hierarchical clustering (Euclidean distance, Ward method) of the top 5% most variable exon junctions was performed.

Identification of sequence mutations

Polymerase chain reaction and bidirectional capillary (Sanger) sequencing of tumor and matched non-tumor DNA was performed to detect sequence mutations in the following genes: *CREBBP*, *CRLF2*, *IKZF1*, *IL7R*, *JAK1*, *JAK2*, *NRAS*, *KRAS*, *NT5C2*, *PAX5* and *TP53*^{16,17} (Beckman Coulter Genomics, Danvers, MA). Primer sequences are provided in Table S18. Primers were designed with M13 forward and reverse tags to facilitate sequencing, and validated using Coriel control DNA to ensure amplification and to allow selection of either the KAPA2G Robust HotStart ReadyMix (KapaBiosystems) or 2x Thermo-Start High Performance ReddyMix (Thermo Scientific) amplification cocktails. Amplification was performed in 10 μ l reaction volumes (4 μ l cocktail, 4 μ l primer, and 2 μ l DNA). Thermal cycling parameters for the KAPA2G cocktail were 95°C for 3 minutes, and 35 cycles of 95°C for 15 seconds, 60°C for 10 seconds and 72 °C for 30 seconds followed by a final incubation of 72 °C for 30 seconds. Thermal cycling parameters for the Thermo-Start cocktail were 95°C for 15 minutes, and 35 cycles of 95°C for 15 seconds, 60 °C for 15 seconds and 72 °C for 1 minute followed by a final incubation of 72 °C for 30 seconds. Samples were PCR amplified, and then purified using Agencourt AMPure XP, and sequenced using ABI GeneAmp 9700 thermal cyclers. The *P2RY8-CRLF2* rearrangement was detected by genomic or reverse transcription with polymerase chain reaction as previously described.^{19,20}

Fluorescence *in situ* hybridization (FISH)

FISH assays were designed to detect 8 chromosomal rearrangements with disruption of various target genes by demonstrating intragenic breakpoints that result in physical separation of the 5' and 3' portions of the target genes, and subsequent fusion of the 3' portion of these genes to different 5' promoter regions. All assays were performed as two sequential hybridization events first using the 5' and 3' target gene specific probes in different colors to demonstrate the presence or absence of intragenic disruption. Imaging was performed following the first hybridization and slide coordinates were recorded. A second hybridization was then performed using the appropriate 5' promoter probe and a second set of images were then made of the previously imaged cells. Using this approach it is possible to identify simultaneous disruption of the target gene and fusion of the differentially regulated 3' end of this gene with a different 5' promoter element.

BAC and fosmid clones corresponding to the appropriate gene targets were obtained from the BACPAC Resource at CHORI (Table S19). All probes were made by nick translation using either Alexafluor 488 dUTP or Alexafluor 594 dUTP. Labeled DNA was combined with sheared human Cot1 DNA and hybridized to denatured slides in a solution containing 50% formamide, 2X SSC, and 10% dextran sulfate at 37°C overnight. Following hybridization the slides were washed once for 5 minutes in 50 formamide and 2X SSC at 37°C. The slides were mounted in Vectashield containing DAPI counterstain and analyzed.

Microscopy was performed using a Nikon E800 widefield fluorescence microscope equipped with a 60X planapochromatic objective, a Photometrics Coolsnap ES camera, an 89400 (Chroma Technologies) multiband pass filter cube and appropriate individual excitation filters mounted in a filter wheel. Nikon NIS Elements software version 4.2 was used to acquire all images.

All images were acquired in 3 colors and in 3 dimensions. Appropriate numbers of planes were determined in order to capture all signals within the cells being imaged and the

spacing between planes was 0.5 μm . After images had been acquired an extended depth of focus function was used in order to combine all FISH signals into a single focused plane. All cells were imaged twice, first after the initial 5' and 3' gene break apart hybridization and then again after the addition of the 3rd probe from the 5' promoter region. Comparing these two sets of images it is possible to identify specific gene break apart that is accompanied by subsequent gene fusion to produce the final oncogenic fusion gene. The first hybridization specifically identifies the allele containing a gene disruption and the second hybridization demonstrates the subsequent fusion of the 5' prime promoter region to the 3' coding region of the disrupted gene. Frequency of gene disruption in specific cases was estimated by analyzing 100 interphase nuclei after the first break apart hybridization.

***In vitro* assays**

Full length fusion transcripts were amplified using HiFi Hot Stat (KAPA Biosystems) or Phusion enzymes, cloned into pCR-Blunt II-TOPO (Life Technologies) and sub-cloned into the MSCV-IRES-GFP retroviral vector. Retroviral supernatants were used to infect murine Ba/F3 or primary *Art^{f/-}* pre-B cells.^{21,22} To evaluate cytokine-independent proliferation, cells were washed three times, seeded in triplicate without cytokine and cell number was recorded daily using a TC10 cell counter (Bio Rad). Drug sensitivity was assessed using the CellTiter-Blue Cell Viability Assay (Promega) according to manufacturer's instructions, and IC₅₀ was determined using nonlinear regression (GraphPad Prism v6.0).

Protein expression

To assess intracellular signaling, cells were harvested at 0.7×10^6 / tube and treated with or without the tyrosine kinase inhibitors dasatinib (100nM) and ruxolitinib (1 μM) for one hour. Cells were fixed, permeabilized and stained with either anti-STAT5 (pY694)-Ax647 (BD Biosciences) or -CRKL (pY207; Cells Signaling Technology) followed by anti-rabbit Pacific Blue conjugated anti-mouse IgG secondary antibodies (Life Technologies). Cells were collected on an LSR II

flow cytometer (BD Biosciences) and analyzed using FlowJo (Tree Star).^{11,23} For immunoblot analysis, cells were lysed in RIPA buffer (Sigma) and 30µg protein was loaded and run on 4-12% NuPage Bis-Tris gels (Life Technologies) at 200V for 1 hour. Blots were probed with anti-ABL1 (24-11), -ABL2 (C20), -IKAROS (H-100), -actin (I-19) (Santa Cruz Technologies), -JAK2 (D2E12) (Cell Signaling Technologies) and -CSF1R (Abcam 37858).

Xenograft models

Xenografts of human Ph-like ALL using NOD.Cg-*Prkdc*^{scid} *Il2rg*^{tm1Wjl}/SzJ (NOD-SCID gamma-null, or NSG) mice²⁴ were established. Mice xenografted with human leukemic cells expressing ETV6-ABL1 were treated with vehicle or dasatinib at 20mg/kg/day by oral gavage 5 days per week.¹¹ Bone marrow harvested from mice xenografted with human leukemic cells expressing ATF7IP-JAK2, IGH-EPOR or ETV6-NTRK3 was used for *ex vivo* cytotoxicity assays as described above.

SUPPLEMENTARY RESULTS

Genomic profiling of Ph-like ALL

Among 54 Ph-like cases analyzed by whole genome or whole exome sequencing, the average number of somatic coding mutations was 21 per case (range 1-107). Forty-four genes were recurrently mutated with 13 genes mutated in at least 3 cases: *PAX5*, *IL7R*, *NRAS*, *KRAS*, *JAK2*, *IKZF1*, *TTN*, *SH2B3*, *FLT3*, *MUC16*, *LTBP1*, *KIF2B* and *BSN*. Incorporating mutations identified by mRNA-seq in 102 additional cases yielded a similar mutation profile (Table S20 and Figure S19).

We also identified multiple non-kinase fusions not previously observed in ALL (27 in 26 cases), several of which involved known targets of rearrangement in ALL, hematopoietic transcription factors and transcriptional regulators or coactivators (e.g. *CBFA2T3*, *EBF1*, *ERG*, *ETV6*, *TCF3* and *PAX5*) and epigenetic modifiers (e.g. the acetyltransferase CREBBP, the histone 3 lysine 36 trimethylase SETD2 and histone demethylase KDM6A (UTX)) (Figure S20). The majority of these cases had additional genetic lesions driving kinase signaling (Table S21) consistent with the notion that deregulation of multiple pathways, including kinase signaling, lymphoid maturation and epigenetic modification contribute to leukemogenesis. Notably, 10 5' fusion partners and 9 3' fusion partners were involved in multiple translocations, indicating these genes are specific targets of rearrangement in Ph-like ALL (Figure S21).

Case descriptions for tyrosine kinase inhibitor treatment of Ph-like ALL

ALL002 with *ETV6-ABL1*

The patient was an 82 year old male who presented with B-ALL and an initial WBC of 183,000. He commenced chemotherapy that was stopped at week 3 because of toxicity. At that time an *ABL1* split was identified by FISH, and *ETV6-ABL1* confirmed by RT-PCR. Based on these molecular results dasatinib was added alone (100 mg daily) with morphological and cytogenetic remission achieved in the bone marrow after 2 weeks of dasatinib treatment. Patient continued

dasatinib daily plus 2 cycles of prednisolone (50 mg orally daily) for 4 weeks each. Remains in cytogenetic remission after 8 months of maintenance dasatinib.

PAWDPK with *FOXP1-ABL1*

The patient was a 9 year-old male who presented with B-ALL and an initial WBC of 26,600. Cytogenetic analysis showed a t(3;9)(p13;q34) and *ABL1* was split on FISH performed to detect *BCR-ABL1* fusion (*BCR* was intact). Ph-like ALL was identified using low density gene expression array (LDA) card and RT-PCR identified a *FOXP1-ABL1* fusion. Dasatinib was added to induction chemotherapy by day 10. The patient is still receiving induction therapy.

PAVZZE with *NUP214-ABL1*

The patient was a 12 year-old male with B-ALL and an initial WBC of 88,000. Cytogenetic analysis showed normal karyotype with 46,XY with additional *ABL1* signals by FISH. SNP array analysis showed amplification of 9q34 suggestive of *NUP214-ABL1* fusion that was confirmed by RT-PCR. He received a 4 drug induction and had 12.4% MRD at the end of induction. After an additional month of consolidation chemotherapy the MRD level was still 0.7% and dasatinib was added to chemotherapy.

PAWALS with *RANBP2-ABL1*

The patient was a 12 year-old male who presented with massive splenomegaly and hyperleukocytosis (905,000 WBC). Cytogenetics showed a t(2;9)(q11.2;q34) and *ABL1* was split on FISH. He initially responded poorly to a 4-drug induction with WBC of 850,000 on day 5. Due to the poor response and *ABL1* disruption, imatinib was added to induction chemotherapy at day 5. At that time, a LDA card gene expression analysis showed the leukemia to be Ph-like and RT-PCR detected a *RANBP2-ABL1* fusion. He cleared peripheral blasts by day 11 and at end induction was in complete remission with normal cytogenetics and *ABL1* FISH. He is currently receiving intensive chemotherapy plus imatinib²⁵ and remains in remission 4 months following diagnosis.

PAVKDX with *RCSD1-ABL1*

The patient was a 6-year-old boy who presented with B-ALL and hyperleukocytosis (107,900 WBC). Cytogenetic analysis showed a t(1;9)(q24;q34), and an *ABL1* split on FISH. Low density array (LDA) card gene expression analysis was positive for Ph-like ALL, and RT-PCR showed *RCSD1-ABL1* fusion. The patient had a poor response to 4-drug induction chemotherapy with end induction MRD 16.4% in the bone marrow. Imatinib was added and bone marrow blasts were 2% at day 29.

PAVYCL with *ZMIZ1-ABL1*

The patient was an 11 year-old female with B-ALL who presented with an initial WBC of 349,200. Cytogenetics were uninformative (46,XX), but *ABL1* was split on FISH performed to detect *BCR-ABL1* fusion (*BCR* was intact). She received a 4-drug induction and end induction MRD was 5.4%. An LDA card study showed the leukemia to be Ph-like and RT-PCR showed *ZMIZ1-ABL1* fusion. Based on the poor response to therapy and the *ABL1* fusion, the treating physician added dasatinib to chemotherapy during consolidation; MRD was 0.88% 3 weeks after dasatinib was added. The patient continues to receive chemotherapy plus dasatinib approximately 6 months after initial diagnosis.

PAVMLC with *RCSD1-ABL2*

The patient was a 5 year-old male with B-ALL and an initial WBC of 57,700. Chromosome analysis showed 47,XXYc and further studies confirmed a diagnosis of Klinefelter syndrome. FISH for *BCR-ABL1* rearrangement was negative, but FISH performed to detect imatinib responsive gene rearrangements showed disruption of *ABL2*. MRD levels were 1.2% after a 4-drug induction. He continued to be MRD positive 6 months into therapy (0.029%). Based on the poor MRD response and *ABL2* rearrangement, imatinib was added at that time. A marrow performed 2 months later showed no MRD and he continues in complete remission approximately one year post-diagnosis, receiving chemotherapy plus imatinib. An LDA card

study showed the leukemia to be Ph-like and RT-PCR showed *RCSD1-ABL2* fusion.

PAVWWX with *ZC3HAV1-ABL2*

The patient was a 6-year-old boy with B-ALL and hyperleukocytosis (170,000 WBC). Cytogenetic analysis showed a t(1;7)(q21;q32). The patient failed to enter remission after a 4-drug induction with end-induction bone marrow blasts of 36% and MRD of 38.5%. Because of the induction failure LDA analysis was performed and showed the case to be Ph-like; RT-PCR showed *ZC3HAV1-ABL2* fusion. Based on these results, dasatinib was added to chemotherapy during the second month of treatment.

ALL021 with *SSBP2-JAK2*

The patient was a 14 year-old male who presented with B-ALL and an initial WBC of 160,000. Cytogenetic studies showed a t(5;9)(q12;p1?3). He had a poor response to 4-drug induction chemotherapy with end induction marrow showing 5.5% blasts by morphology and MRD. He received 2 weeks of extended induction therapy and repeat BM showed 2% blasts. An LDA card study was not performed due to lack of material, but RT-PCR performed on bone marrow showed *SSBP2-JAK2* fusion. Based on the molecular results, the patient began standard consolidation chemotherapy with addition of ruxolitinib (20 mg/m²/dose). A bone marrow performed 3 weeks later showed 1% MRD and end consolidation bone marrow showed 0.3% MRD. Ruxolitinib has been held intermittently due to thrombocytopenia.

PAVZXA with *EBF1-PDGFRB*

The patient is a 14 year-old male who presented with B-ALL and an initial WBC of 41,700. Cytogenetics showed trisomy 5. He received a 4-drug induction, but failed to enter remission with end induction MRD 25.0%. Because of the induction failure an LDA card study was performed and showed the leukemia to be Ph-like; multiplex RT-PCR showed *EBF1-PDGFRB*, which was confirmed by repeat RT-PCR and bidirectional Sanger sequencing. He received consolidation therapy with clofarabine, cyclophosphamide and etoposide with dasatinib added

based upon molecular data. He achieved an MRD negative remission and remains in remission about 5 months post-diagnosis with plans to undergo matched sibling BMT.

PAVMJD with *EBF1-PDGFRB*

The patient was a 6 year old male who presented with B-ALL and an initial WBC of 244,400. He received 4-drug induction chemotherapy but failed to enter remission with day 29 marrow showing 44% blasts. Cytogenetics were normal, however FISH was positive for *PDGFRB* break apart and *EBF1-PDGFRB* fusion confirmed by RT-PCR. Imatinib was commenced with 3 courses of intensified salvage therapy. (MRD 0.38%). Patient received matched sibling donor HSC transplant and switched to dasatinib with 0.08% MRD at day 30 post-transplant, and negative MRD day 191 post-transplant.

ALL024 with *EBF1-PDGFRB*

The patient was a 7 year old Latino male who presented with B-ALL and initial WBC of 600,000. He failed to enter remission with 4 drug induction (90% blasts at day 23), and showed testicular involvement. SNP array showed deletion of *IKZF1* deletion and gains in 5q32 and 5q33.3 that interrupted the *PDGFRB* and *EBF1* loci, respectively. FISH studies demonstrated an extra *PDGFRB* signal with suspect *EBF1-PDGFRB* that needs molecular confirmation. Imatinib, cyclophosphamide and etoposide were commenced with MRD 4.3% after 1 month. Imatinib dose was increased with MRD 0.44% after additional month of treatment. MRD was 0.0226% after two months of dasatinib treatment, and the patient proceeded to matched unrelated donor hematopoietic stem cell transplantation.

SUPPLEMENTARY FIGURES

Figure S1. CONSORT diagram of B-ALL cases included in the study

Cases included in childhood National Cancer Institute (NCI) standard-risk (SR; age 1-9 years and peripheral blood leukocyte count at diagnosis $<50,000/\mu\text{l}$), childhood NCI high-risk (HR; age 10-15 years and/or leukocyte count $\geq 50,000/\mu\text{l}$), adolescents (age 16-20 years) and young adults (age 21-39 years). Samples were obtained from patients treated on St Jude Children's Research Hospital (St Jude), the Children's Oncology Group (COG), the Eastern Cooperative Oncology Group (ECOG), MD Anderson Cancer Center (MDACC), and the Alliance – Cancer and Leukemia Group B protocols (CALGB).

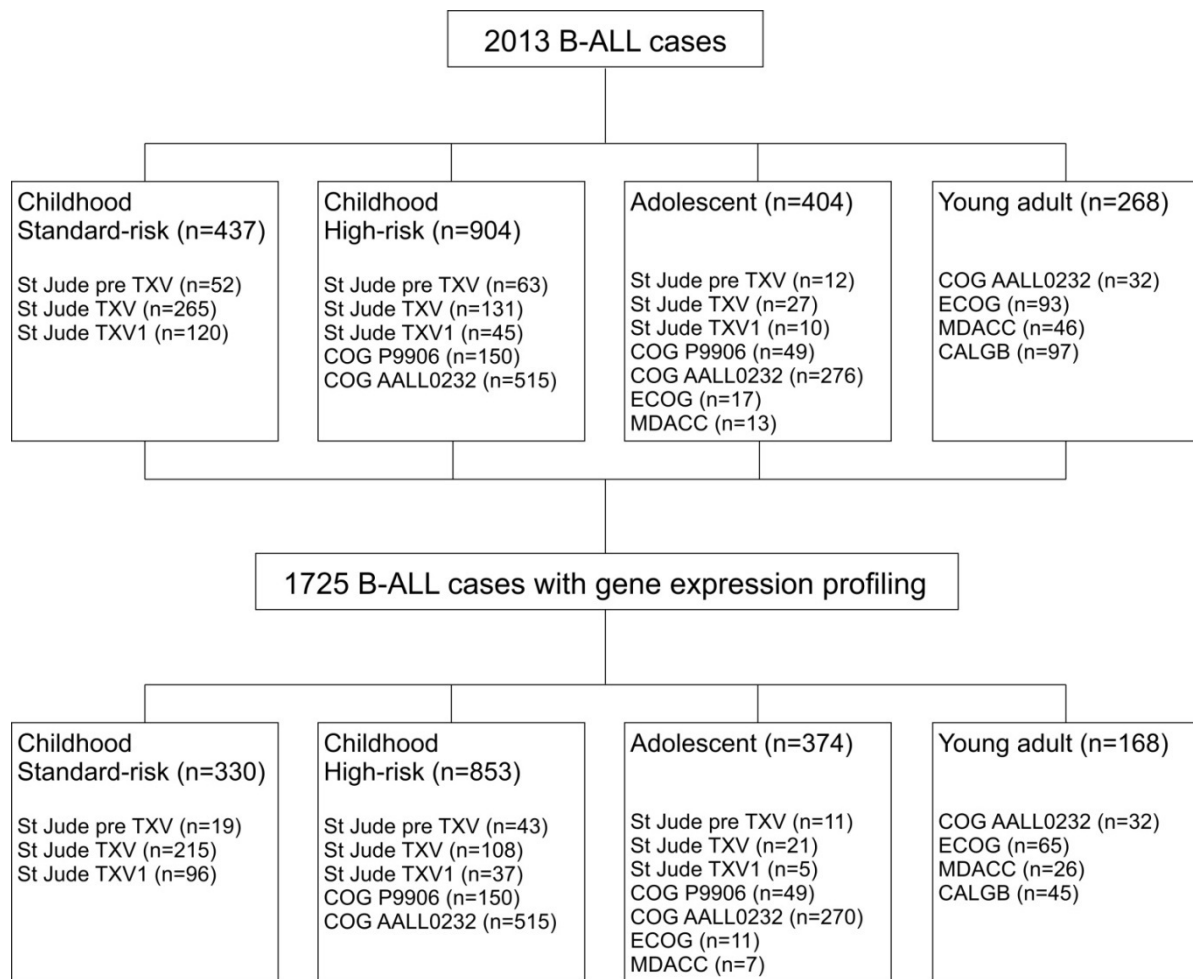


Figure S2. Detailed outcome analyses of childhood, adolescent and young adult ALL

Kaplan-Meier estimates for event-free (Panel A) and overall survival (Panel B) in children with high-risk B-ALL, adolescents and young adults with B-ALL according to *BCR-ABL1*, *MLL*-rearranged, Ph-like and all other B-ALL genotypes (including *ETV6-RUNX1*, *E2A-PBX1*, hyperdiploid, hypodiploid and other). A) The 5-year event-free survival for patients with Ph-like B-ALL is inferior to other B-ALL in children with high-risk B-ALL (58.2 ± 5.3 vs. 83.9 ± 1.5 ; $P < 0.001$), adolescents (41.0 ± 7.4 vs. 83.3 ± 3.6 ; $P < 0.001$) and young adults (24.1 ± 10.5 vs. 63.1 ± 9 ; $P < 0.001$). B) The 5-year overall survival for patients with Ph-like ALL is inferior to other B-ALL in children with high-risk B-ALL (72.8 ± 4.8 vs. 92.1 ± 1.1 ; $P < 0.001$), adolescents (65.8 ± 7.1 vs. 92.5 ± 2.5 ; $P < 0.001$) and young adults (25.8 ± 9.9 vs. 75.4 ± 8.2 ; $P < 0.001$). EFS, event-free survival; HR, high-risk; OS, overall survival.

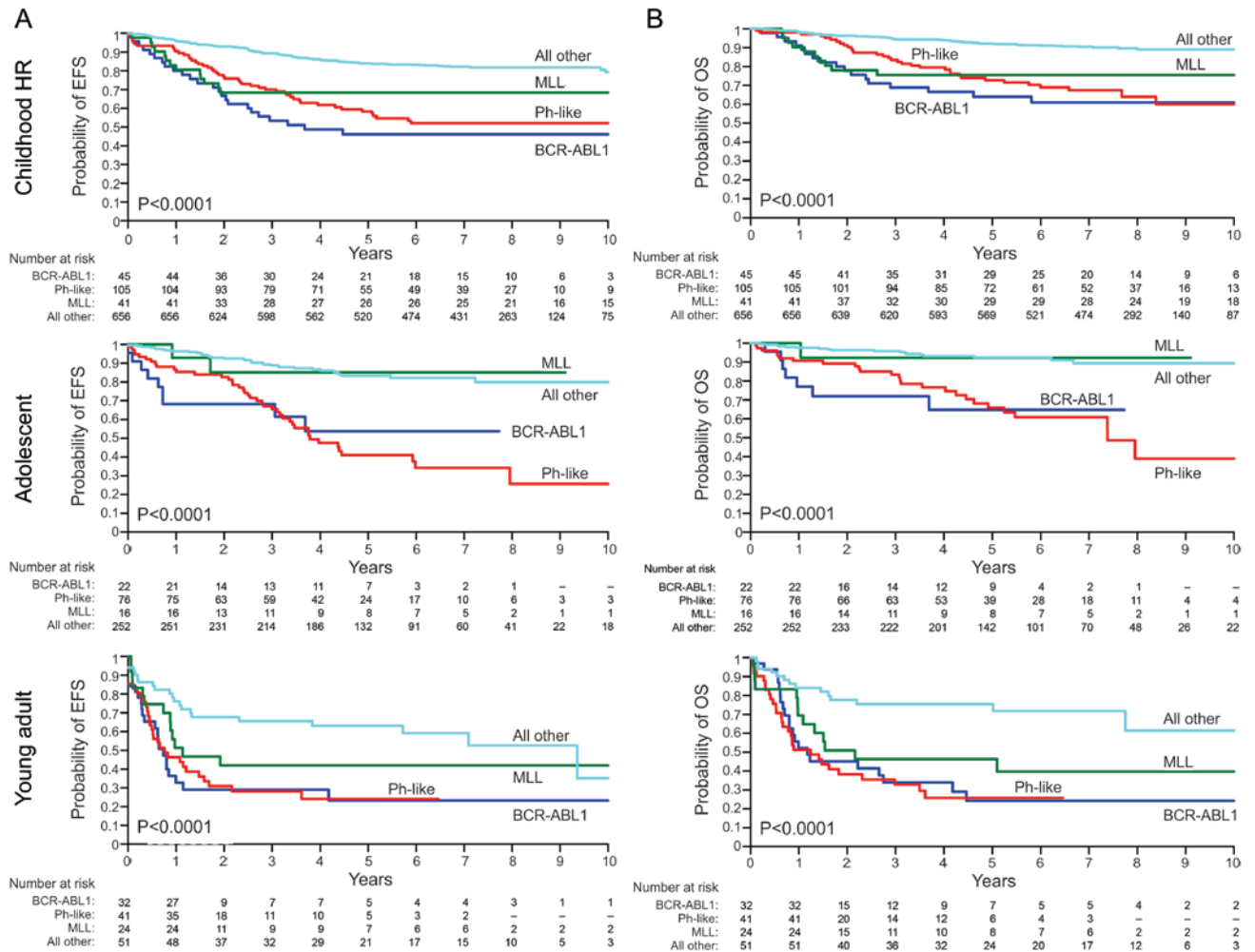


Figure S3. Janus kinase mutations

Protein domain plots for *JAK* mutations in *CRLF2*-rearranged Ph-like cases. FERM, band 4.1 ezrin, radixin, and moesin domain; SH2, Src homology 2 domain; SH2, Src homology 2 domain.

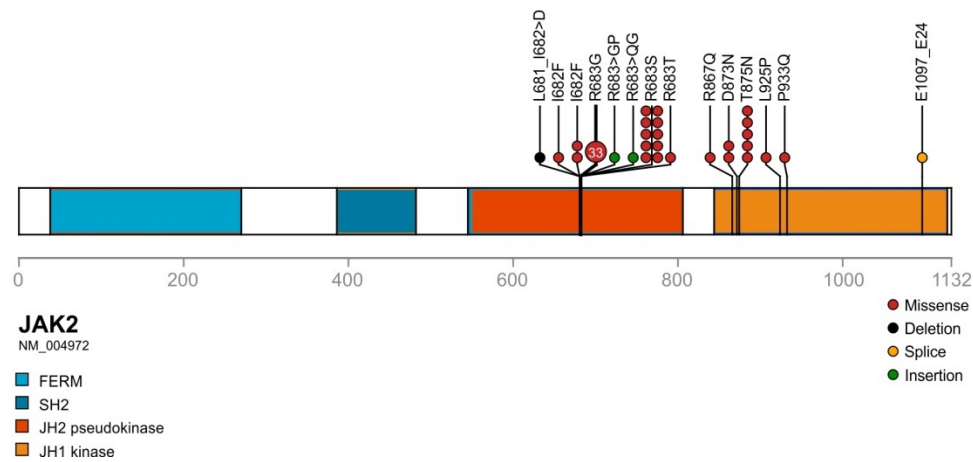
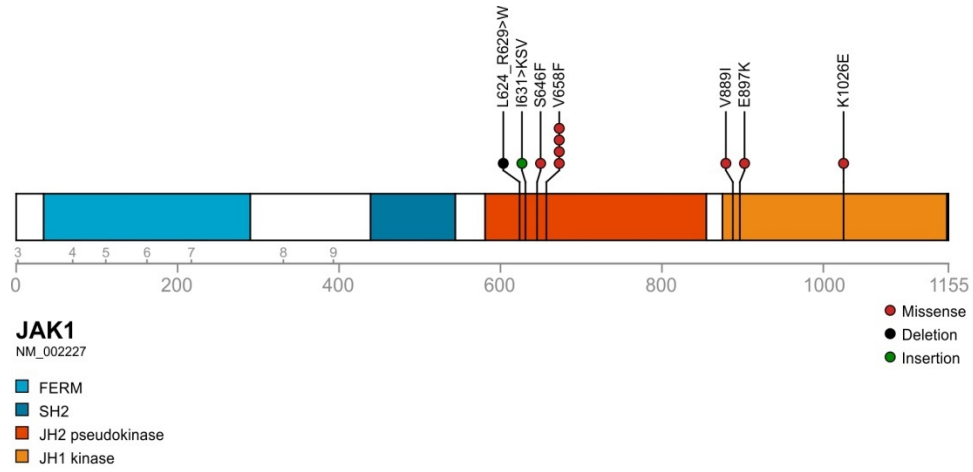


Figure S4. Microarray gene expression profiling

Hierarchical clustering of microarray gene expression data using 340 genes identified by ROSE¹³ for 1181 cases studied using Affymetrix U133 Plus 2.0 arrays showing co-clustering of Ph-like (pink bars) and BCR-ABL1-positive cases (red bars).

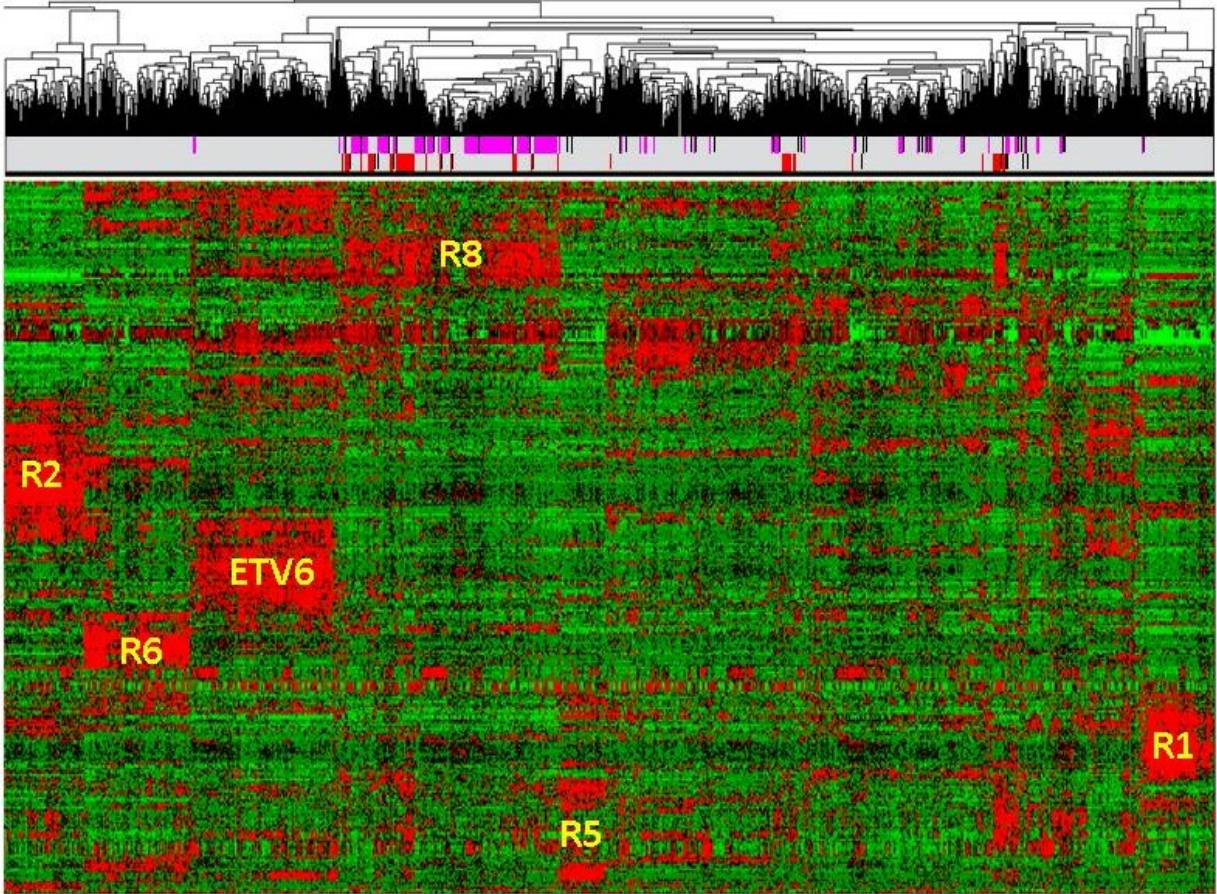


Figure S5. Principal components analysis of mRNA-seq data

Principal component analysis of FPKM mRNA-seq gene expression data showing co-clustering of BCR-ABL1 positive and Ph-like cases. The hypodiploid case clustering with *ETV6-RUNX1* cases harbors a *dic(7;12)(p11.2;p11.2)* and *AMPH-ETV6* fusion.

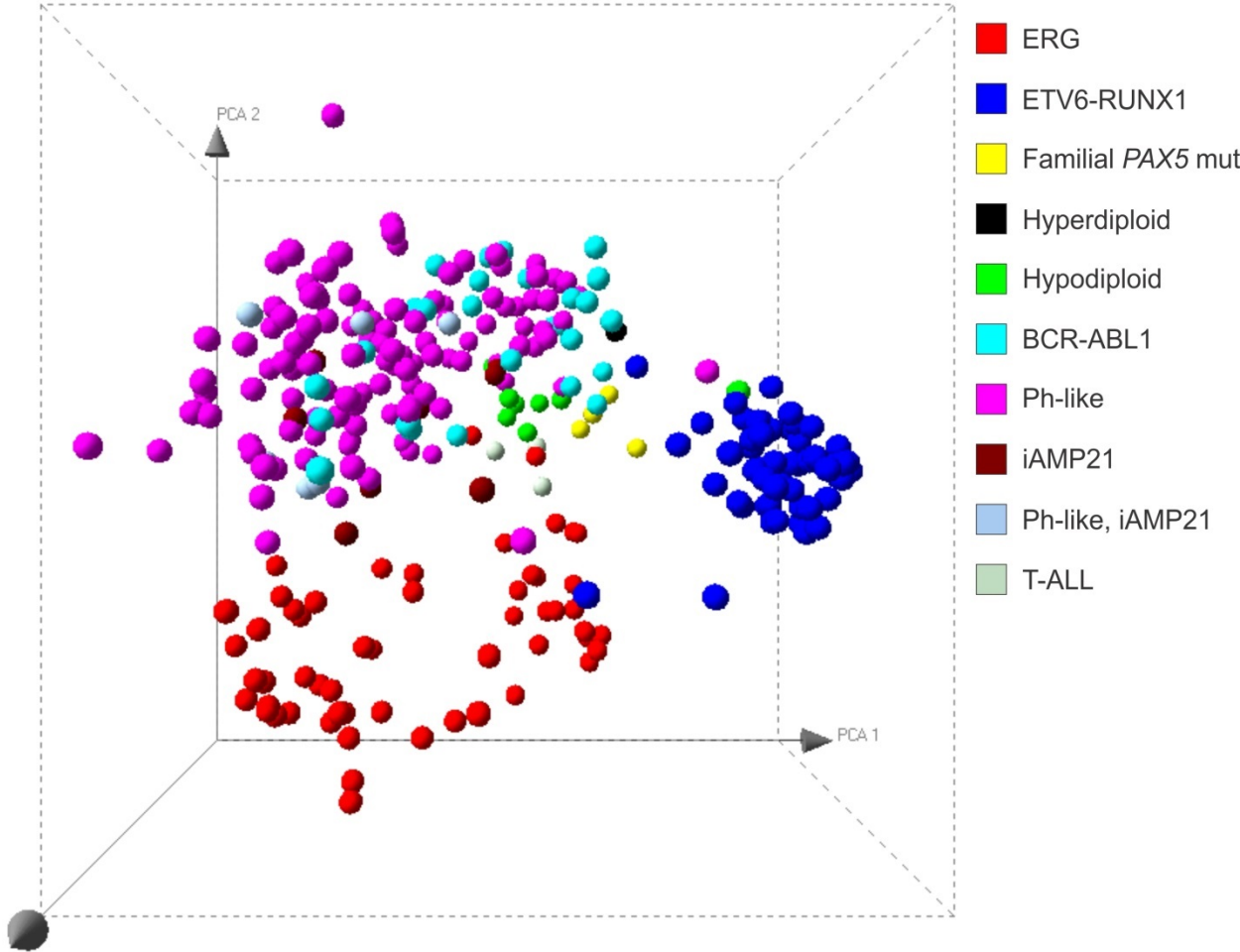


Figure S6. Recurring kinase, B-cell pathway and tumor suppressor pathway alterations in Ph-like ALL

Data are shown for 154 Ph-like ALL cases subjected to next-generation sequencing including mRNA-seq, whole genome sequencing (WGS), and/or whole exome sequencing (WES). For details of specific alterations see Tables S9, S12 and S20.

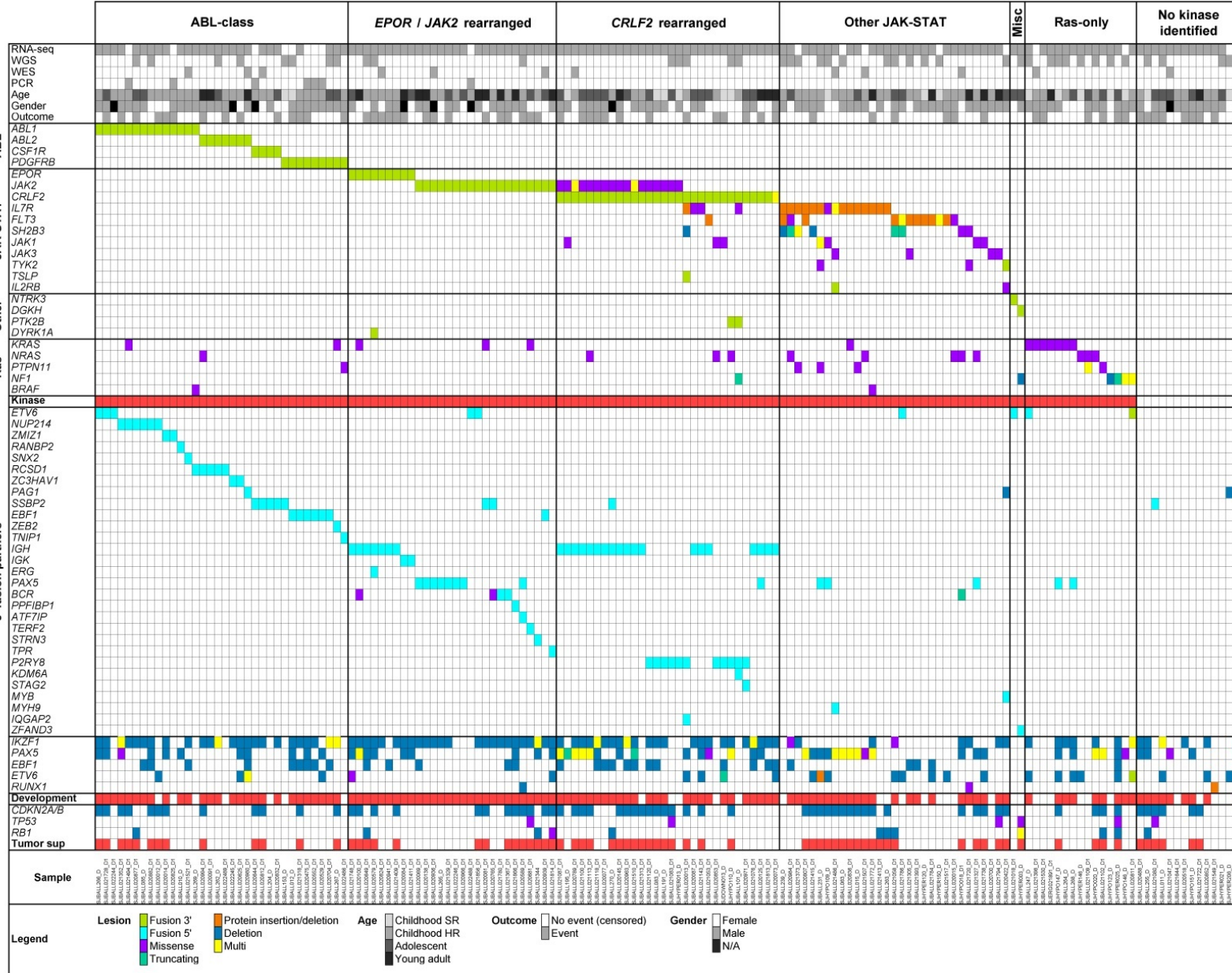


Figure S7. Frequency of Ph-like ALL subtypes in childhood high-risk (HR), adolescents and young adults

Panel A shows the breakdown of Ph-like ALL into *CRFL2*-rearranged *JAK* mutant, *CRFL2*-rearranged *JAK* wild-type (WT), all other kinase lesions and unknown. Panel B shows the breakdown of “Other kinase lesion” into the indicated subgroups based on genetic alteration. *ABL1*-class (*ABL1*, *ABL2*, *CSF1R* and *PDGFRB*); Other *JAK*-*STAT* (*FLT3*, *IL7R*, *SH2B3*, *JAK1/3*, *TYK2*, *IL2RB* and *TSLP*); *Ras* (*KRAS*, *NRAS*, *NF1*, *PTPN11* and *BRAF*). HR, high-risk.

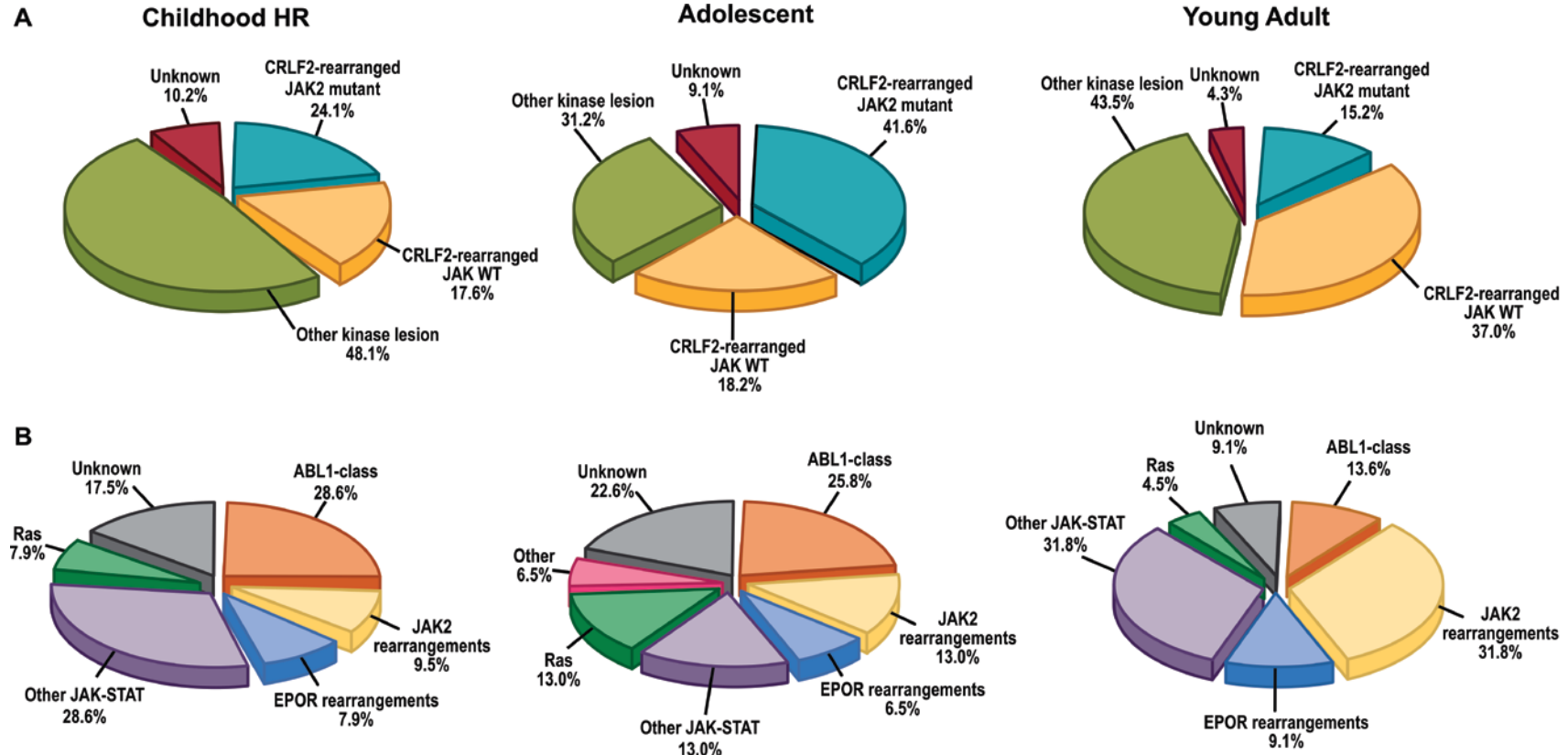
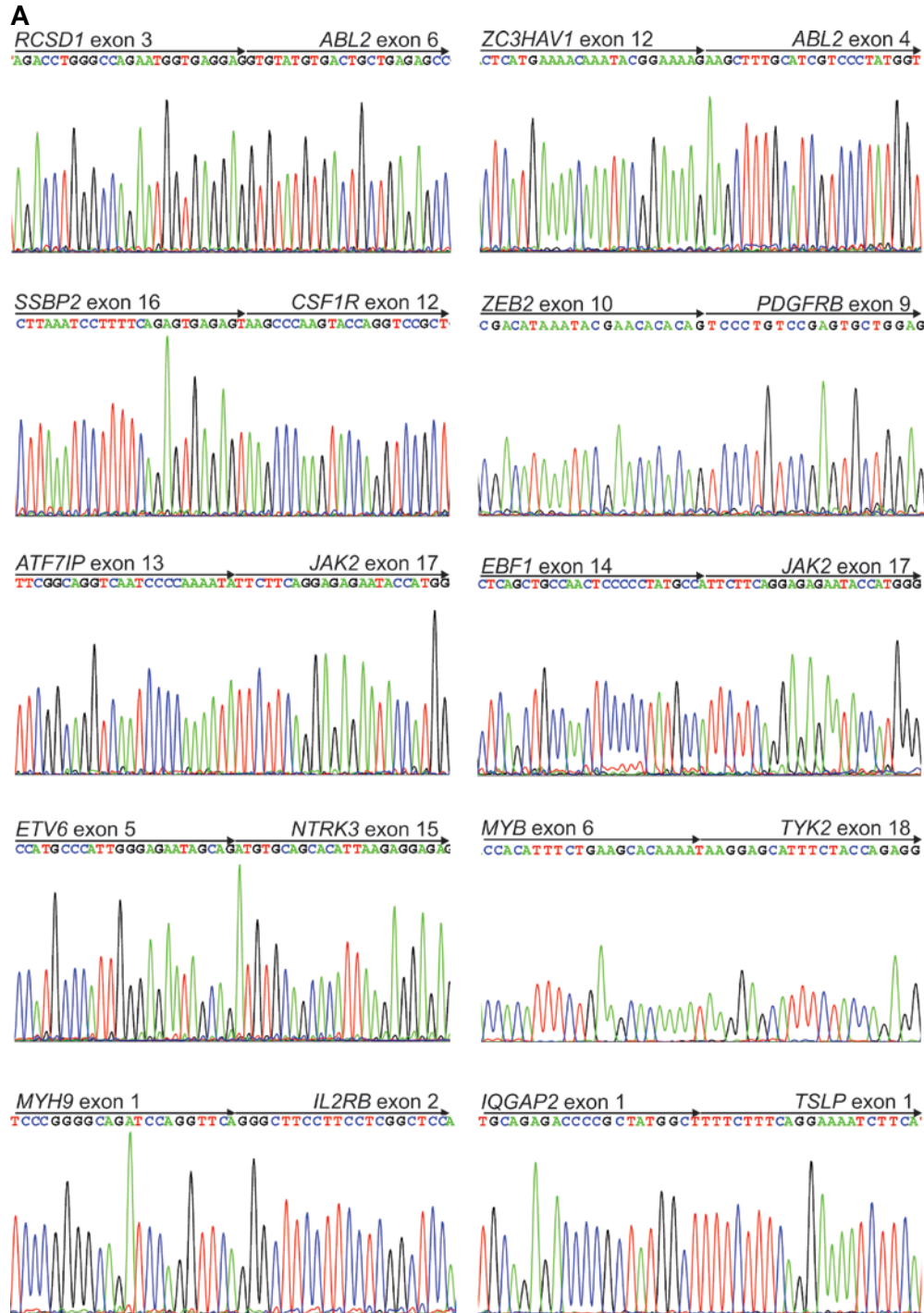
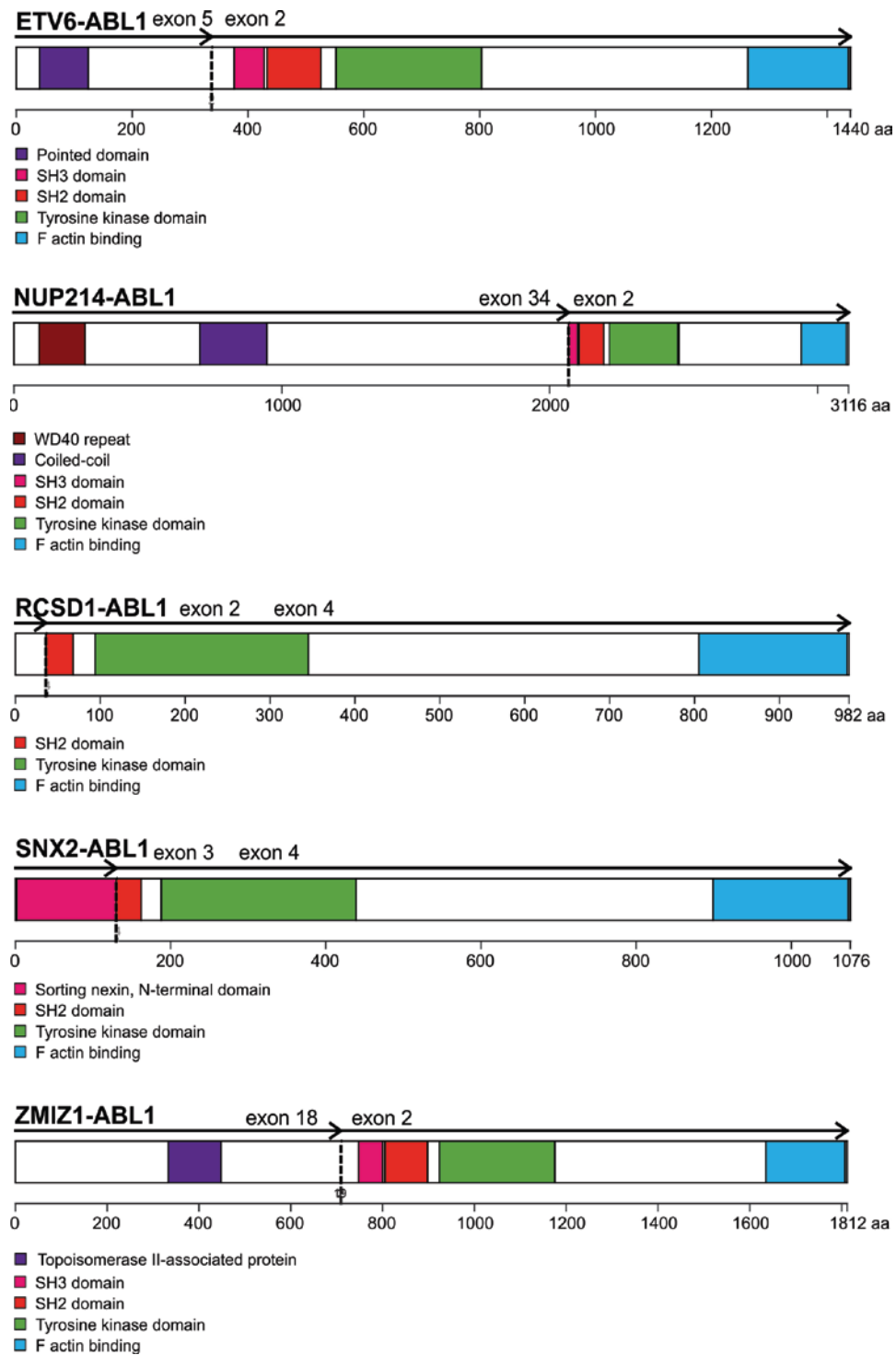


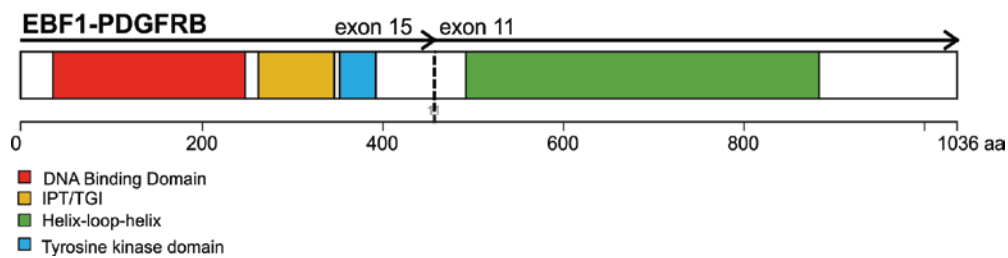
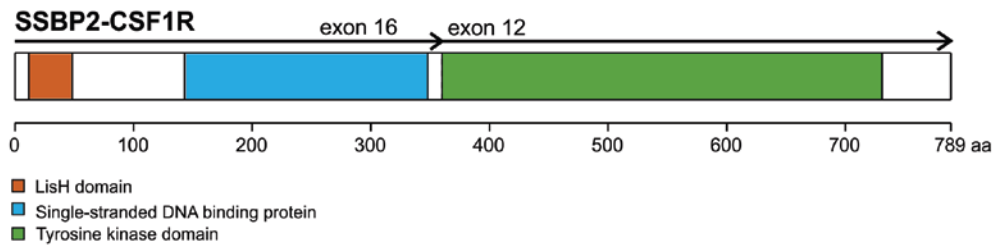
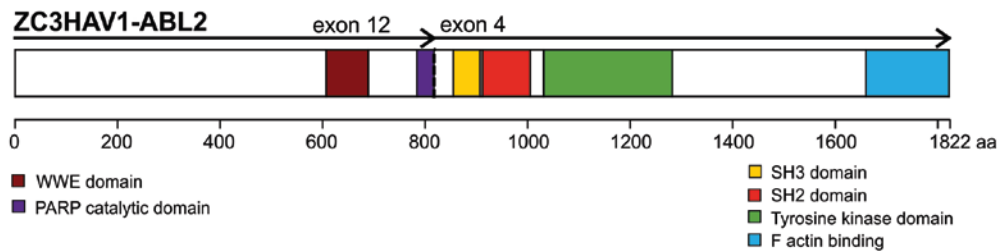
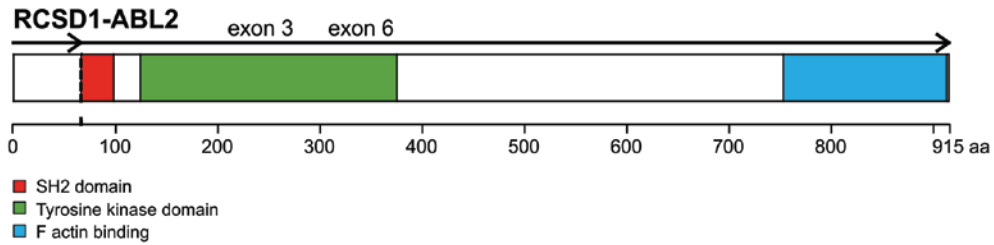
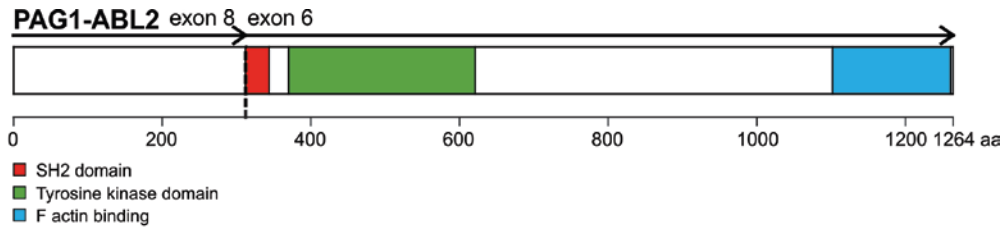
Figure S8. Kinase fusions in Ph-like ALL

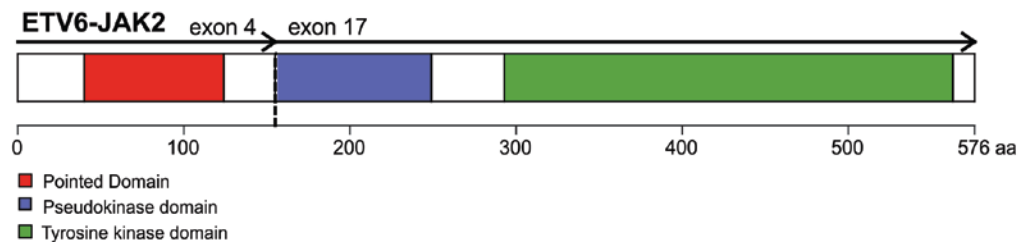
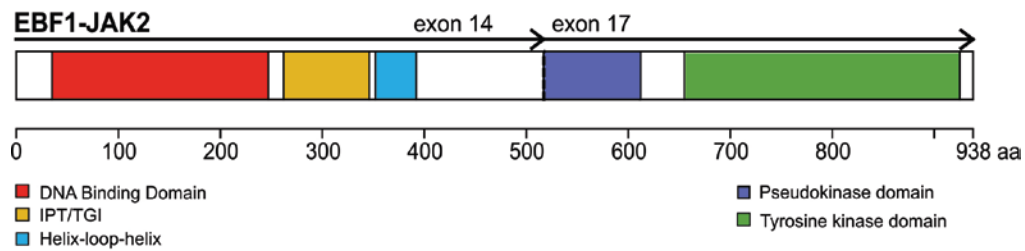
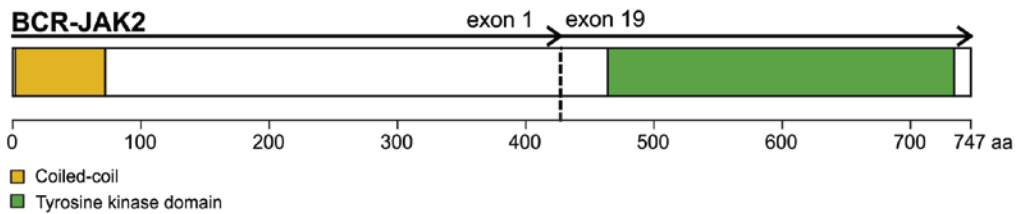
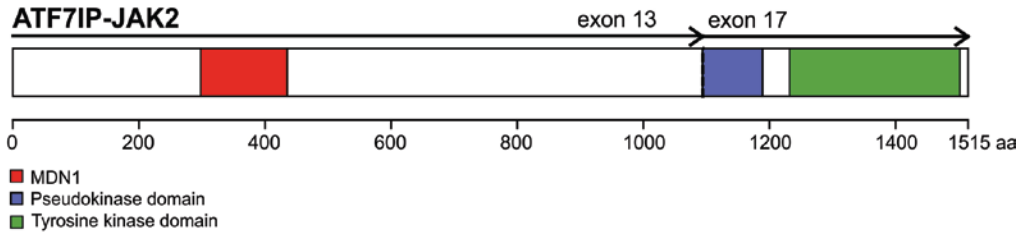
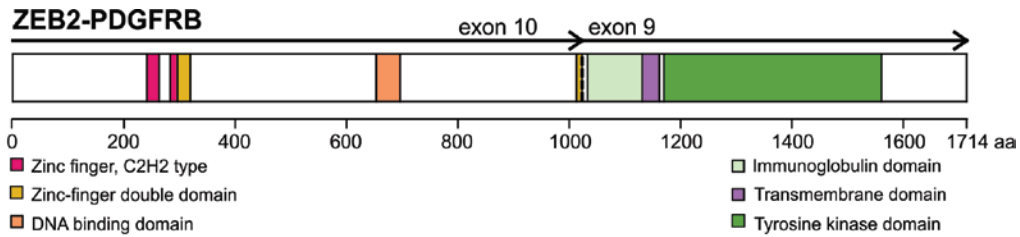
A) Sanger sequencing validation and B) protein domain plots of kinase fusions in Ph-like ALL. All kinase fusions retain an intact tyrosine kinase domain. IPT/TIG, immunoglobulin-like fold, plexins, transcription factors / transcription factor immunoglobulin; LisH, Lis Homology; SH, Src homology domain; TRFH, telomeric repeat binding factor.



B







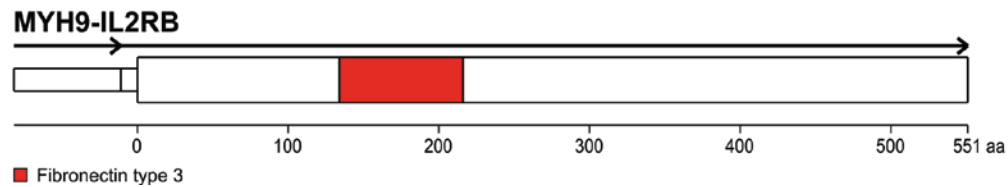
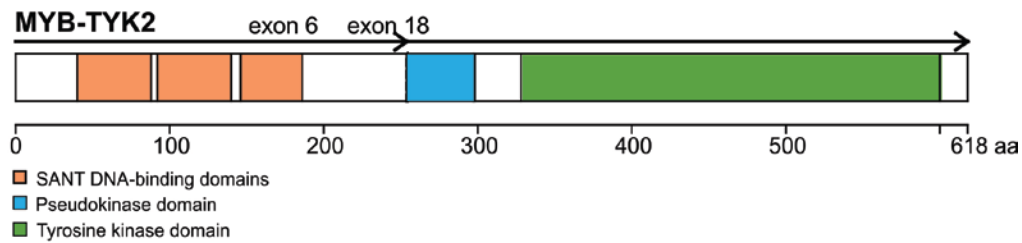
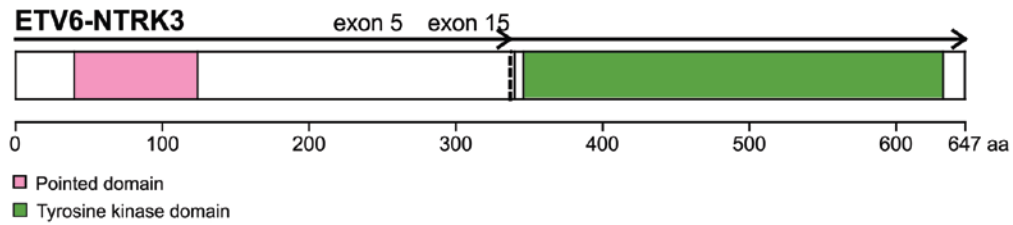
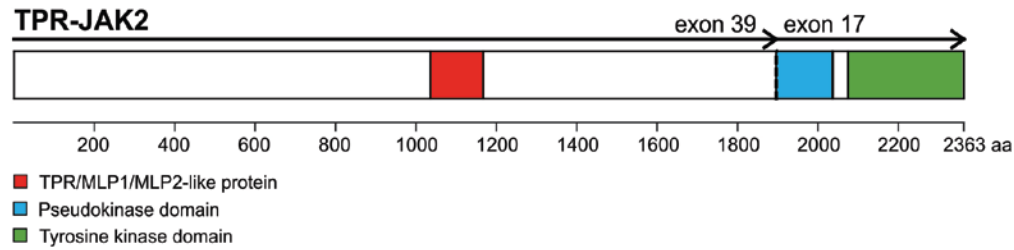
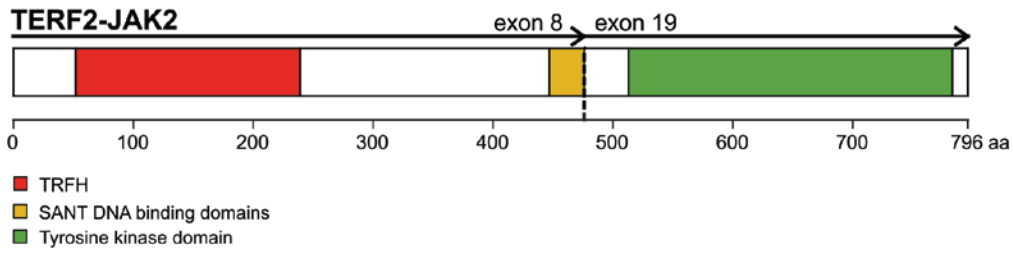
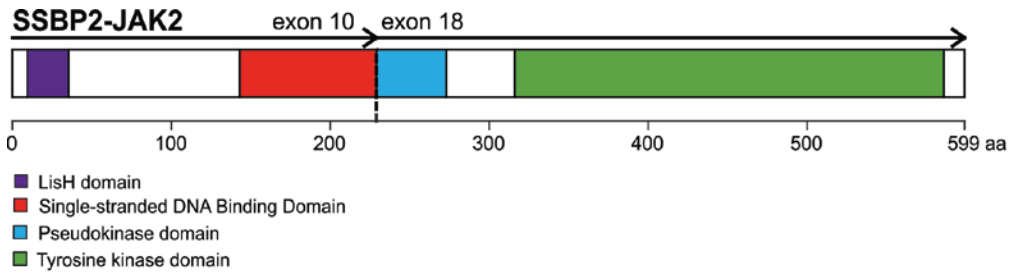


Figure S9. Fluorescence *in situ* hybridization (FISH) of kinase fusions

A) The probe in the 5' region of *JAK2* is red and 3' region is green. One *JAK2* allele of this gene is intact (contiguous red and green signals) and the other is split (left). Second hybridization showing 5' of *BCR* (red) fused to the split *JAK2* allele (right). *JAK2* 3' co-localizes with the 5' region of *ETV6* (B), *PAX5* (C), *PPFIBP1* (D) *SSBP2* (E) and *TPR* (F). *ABL2* 3' co-localizes with the 5' region of *RCSD1* (G). H) Break-apart of *EPOR* (left). Fusion of *IGH* (green) to 3' of *EPOR* (right). Refer to Table S19 for probe details.

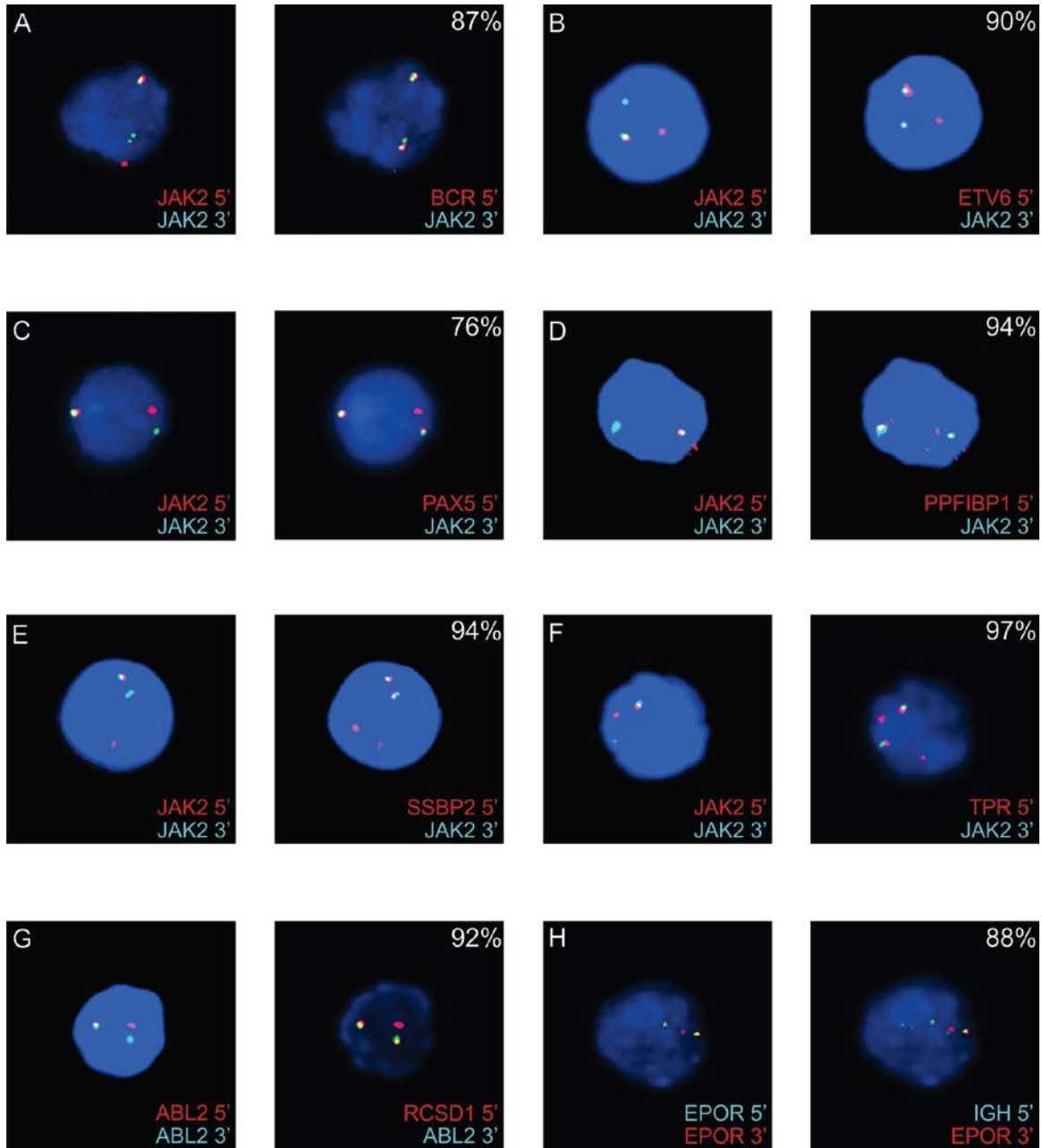





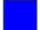


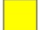











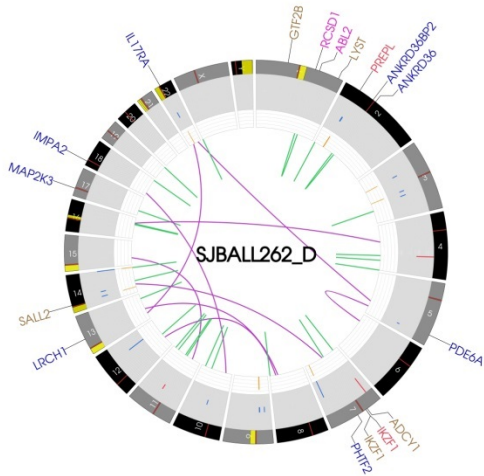
Figure S10. CIRCOS plots

Representative CIRCOS plots of cases studied by whole genome sequencing. Depicted are sequence mutations and structural variants (SV) including DNA copy number variations (CNV), intrachromosomal and interchromosomal translocations. LOH, loss of heterozygosity; UTR, untranslated region.

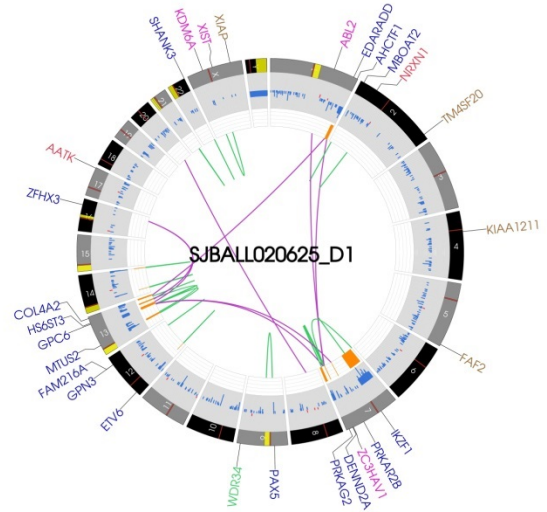
CIRCOS legend

LOH	SV	CNV	Mutations
 LOH	 Gene	 Gene	 Splice
	 Intra	 Loss	 Exon
	 In frame gene fusion	 Fusion	 UTR
	 Interchromosomal		 Intron
			 Nonsense
			 Missense
			 Silent
			 Protein Deletion
			 Protein Insertion
			 Frameshift

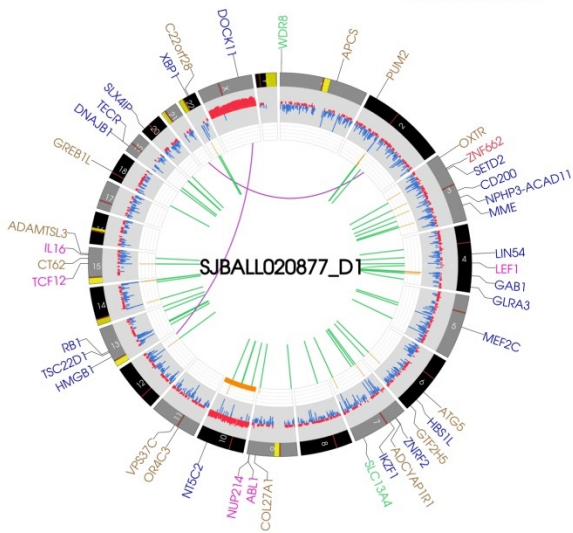
B: ABL1/ABL2 rearranged cases



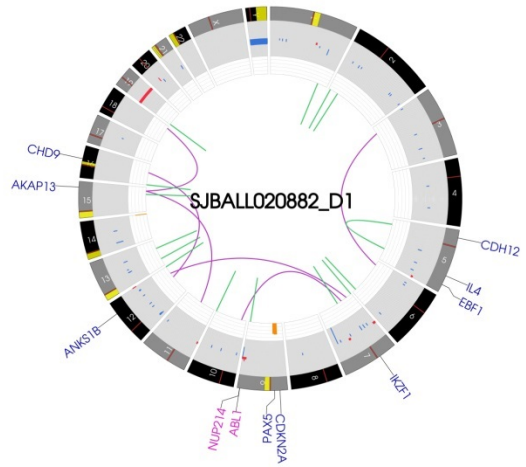
RCS1-ABL2



ZC3HAV1-ABL2

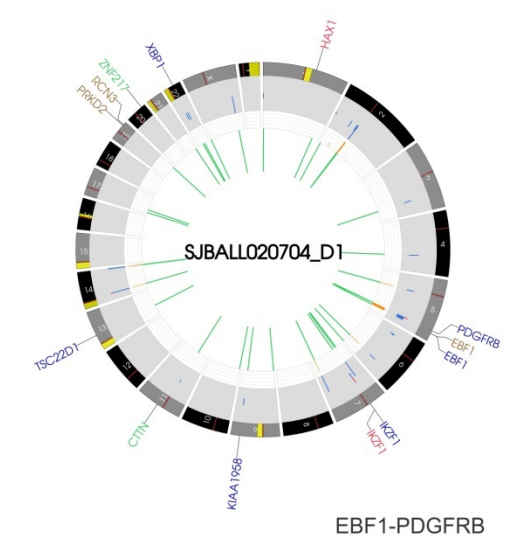
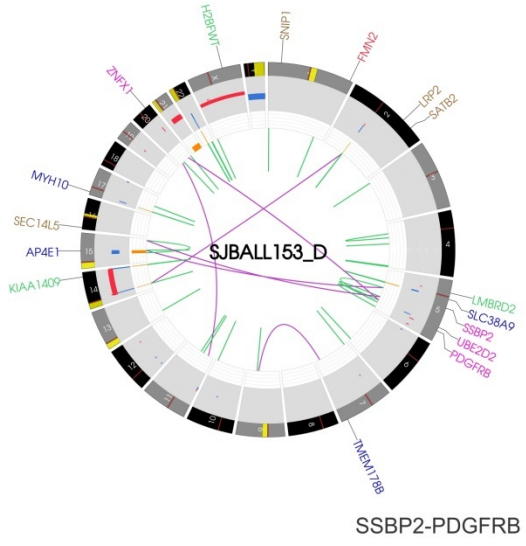
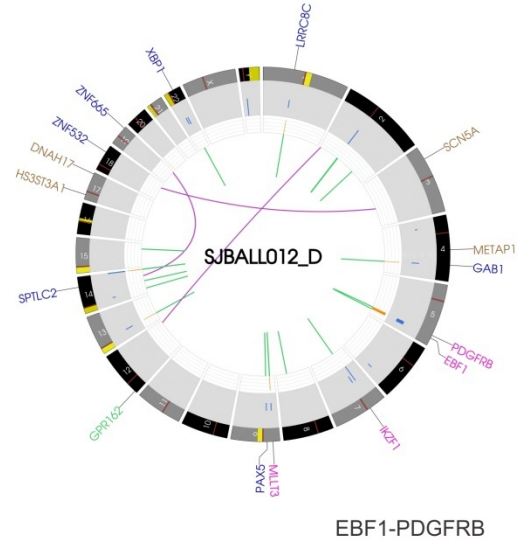
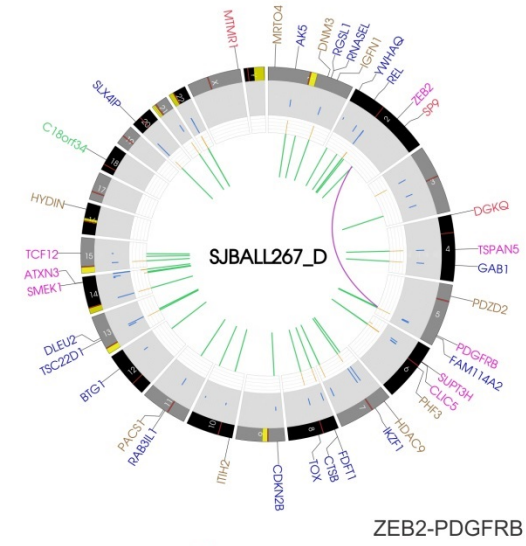


NUP214-ABL1

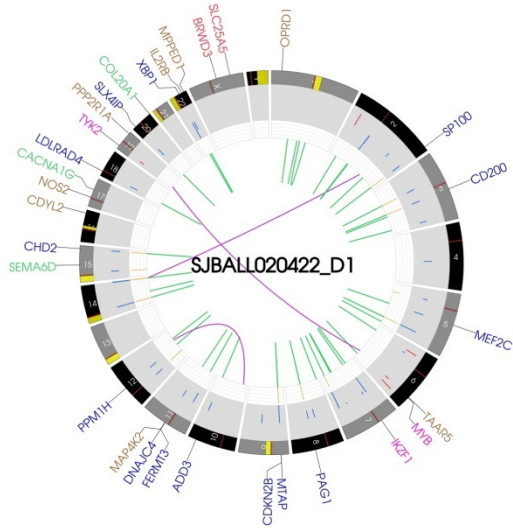


NUP214-ABL1

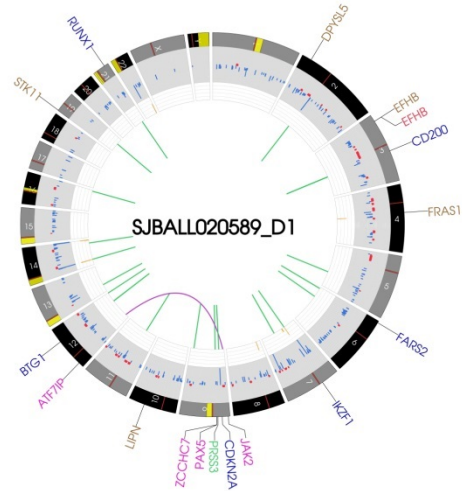
C: PDGFRB-rearranged cases



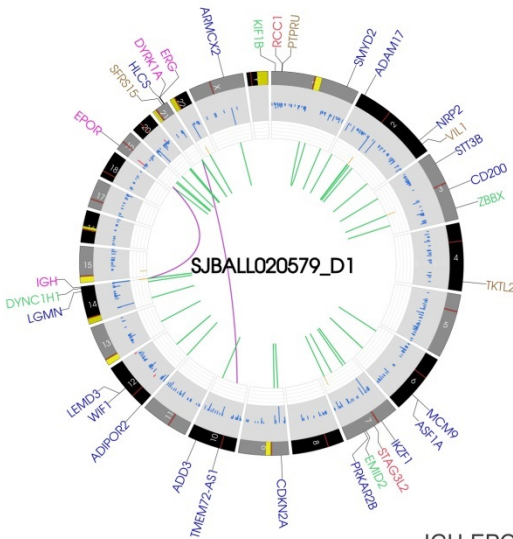
D: TYK2, JAK2 and EPOR-rearranged cases



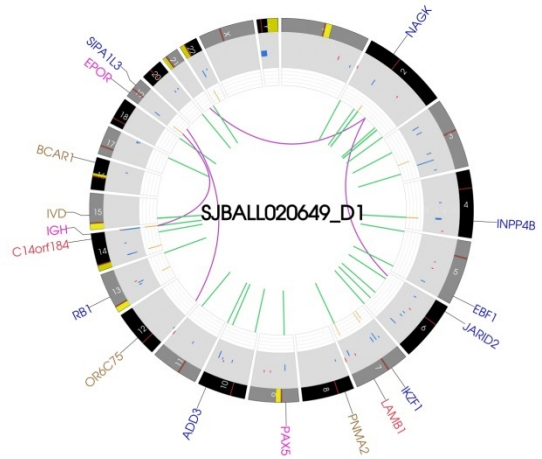
MYB-TYK2



ATF7IP-JAK2



IGH-EPOR



IGH-EPOR

Figure S11. Ras pathway mutations

Protein plots of Ras pathway mutations in Ph-like ALL.

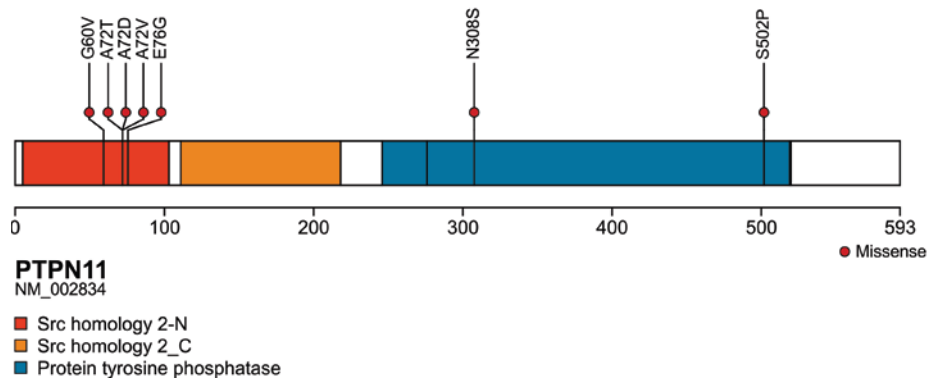
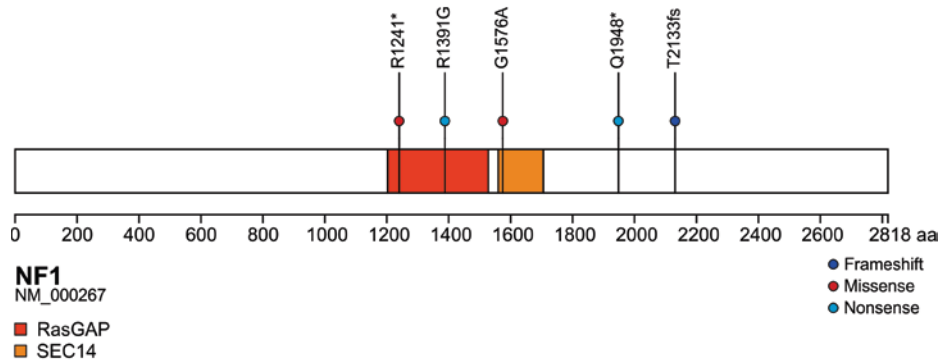
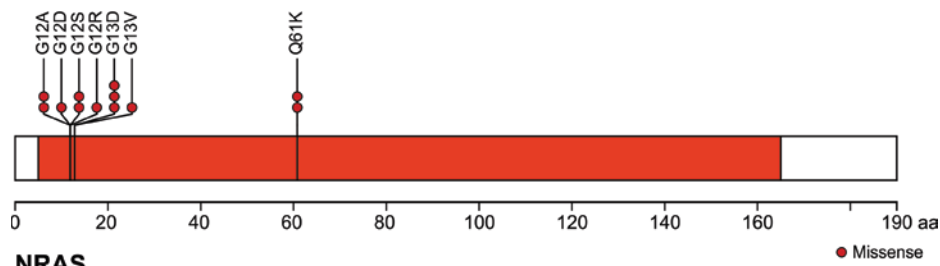
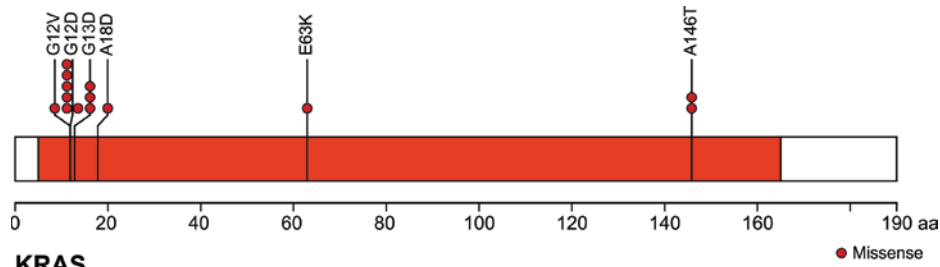
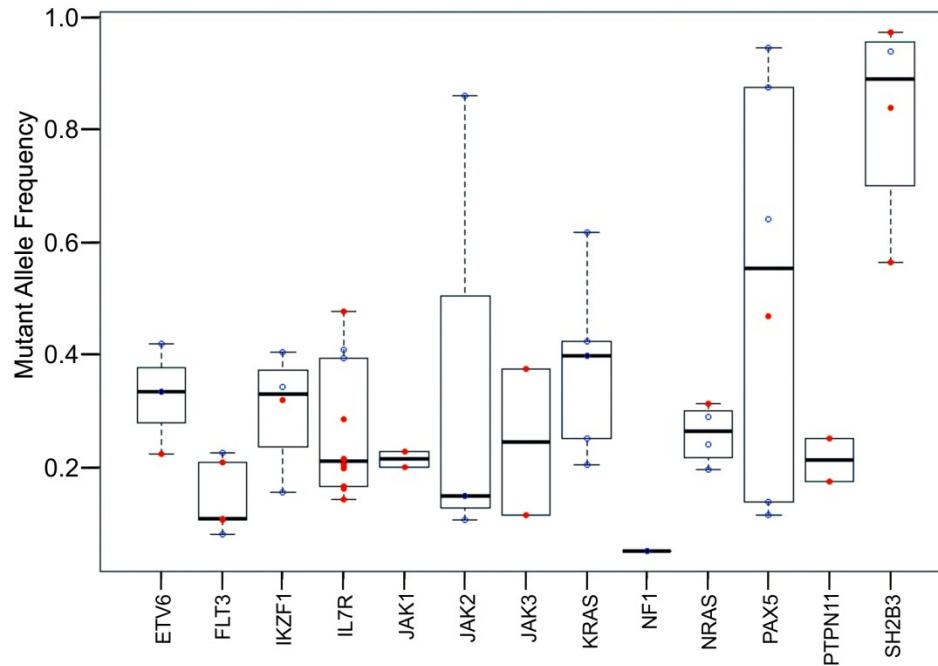


Figure S12. Subclonal mutations in Ph-like ALL.

A) Mutation allele frequency of the most recurrently mutated genes identified in the 54 cases analyzed by whole genome or whole exome sequencing. Mutations in *FLT3*, *IL7R*, *JAK1*, *JAK2*, *JAK3*, *NF1*, *NRAS*, and *PTPN11* were subclonal, and several cases harbored multiple subclonal mutations in the same pathway, indicating the presence of multiple subclones with distinct mutations activating JAK-STAT or Ras signaling. Refer to Table S14 for case details. The red dots represent cases that lack kinase fusions. B) Proportion of variants in each case subjected to whole genome sequencing that are clonal (MAF \geq 0.4) or subclonal. MAF, mutant allele frequency.

A



B

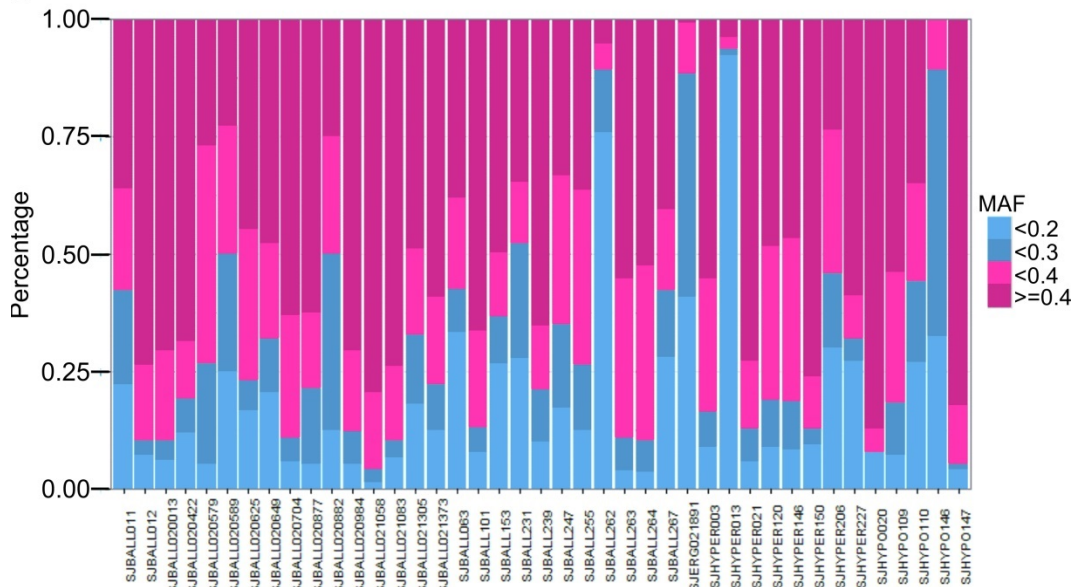
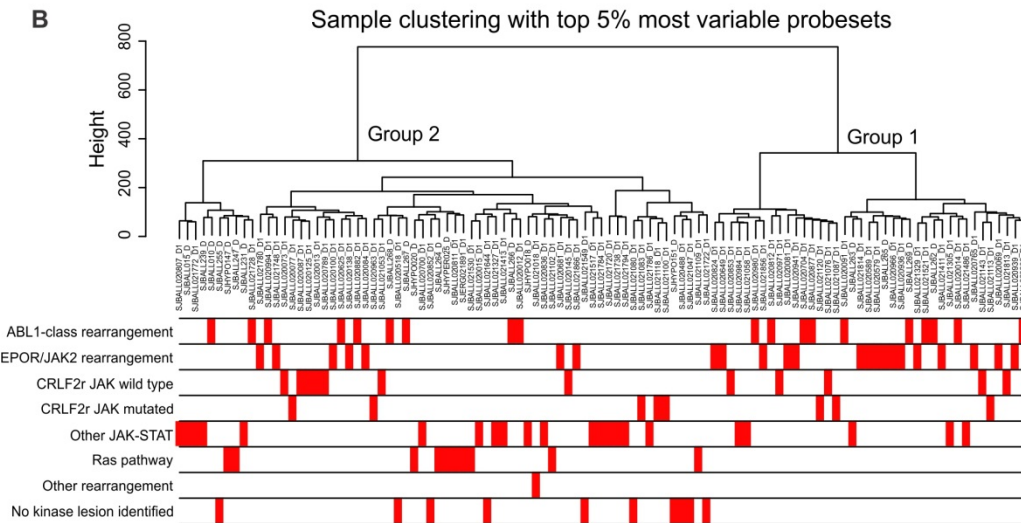
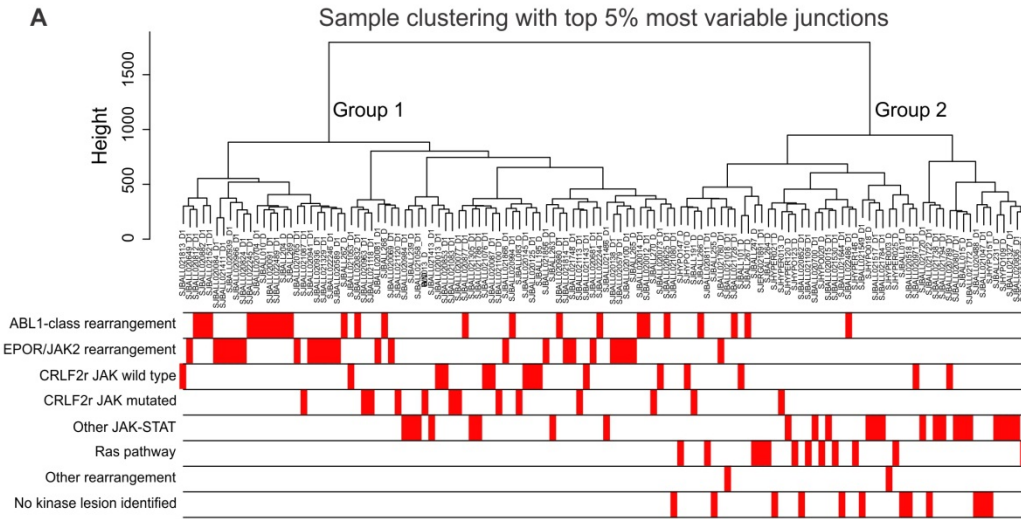


Figure S13. Clustering of Ph-like ALL subgroups

A) Sample clustering using the top 5% most variable junction reads from RNA-seq data and B) top 5% most variable genes from Affymetrix U133A Plus 2.0 microarray data. C) The Fisher exact test to calculate lesion enrichment for RNA-seq data. ABL-class, EPOR and JAK2 rearrangements are enriched in group 1, Other JAK-STAT and Ras-only cases are enriched in group 2.



C

Ph-like group	Total cases	Group 1 N (%)	Group 2 N (%)	P value
ABL1-class rearrangement	24	20 (83.3%)	4 (16.7%)	0.01
EPOR/JAK2 rearrangement	24	23 (95.8%)	1 (4.2%)	<0.001
CRLF2r JAK2 wild-type	15	11 (73.3%)	4 (26.7%)	0.27
CRLF2r JAK2 mutant	13	11 (84.6%)	2 (15.4%)	0.07
Other JAK-STAT	24	8 (33.3%)	16 (66.7%)	<0.001
Ras pathway	12	0 (0%)	12 (100%)	<0.001
Other fusion	2	0 (0%)	2 (100%)	0.168
No kinase lesion identified	12	1 (9.10%)	11 (90.9%)	<0.001

Figure S14. Outcome analyses between different subgroups in Ph-like ALL

Kaplan-Meier estimates for event-free (Panel A) and overall survival (Panel B) in children with standard-risk and high-risk B-ALL, adolescents and young adults with B-ALL according to Ph-like genetic subgroup as indicated. There are significant differences in 5 year event-free survival, with *JAK2/EPOR* rearranged cases (26.1 ± 8.5) and *CRLF2*-rearranged *JAK2* mutant cases (38.8 ± 7.0) having a poor prognosis, whilst cases harboring Other *JAK-STAT* (68.3 ± 9.9) and *Ras* pathway only alterations (85.7 ± 11.5) have a more favorable outcome. Refer to Table S15 for analysis. WT, wild-type.

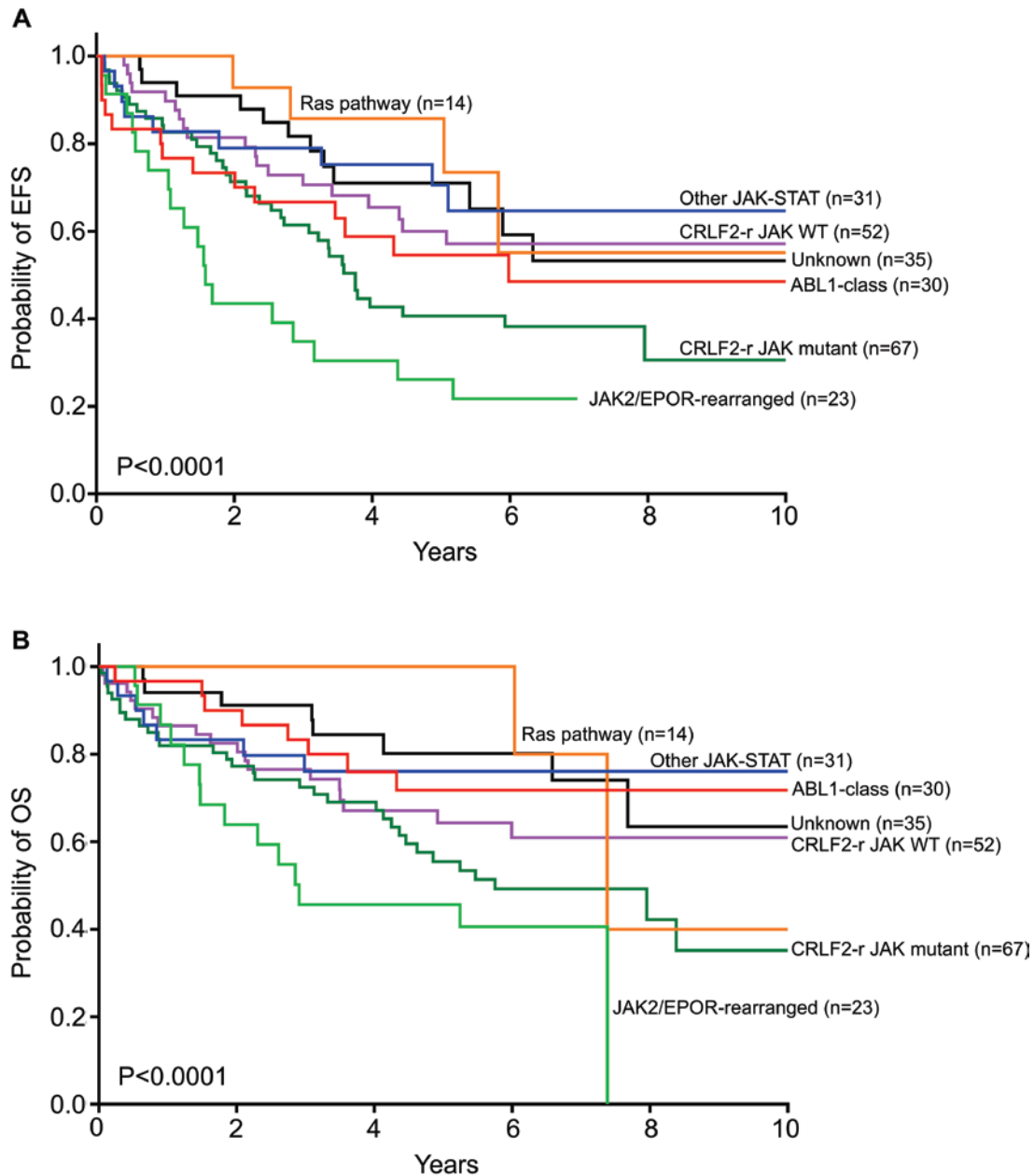


Figure S15 Outcome analyses for *IKZF1* alteration

Kaplan-Meier estimates of event-free (Panel A) and overall survival (Panel B) broken into subgroups: Ph-like *IKZF1* altered, Ph-like *IKZF1* wild type (WT), non Ph-like *IKZF1* altered, non Ph-like *IKZF1* WT for childhood high-risk ALL, adolescents and young adults. EFS, event-free survival; HR, high-risk; OS, overall survival.

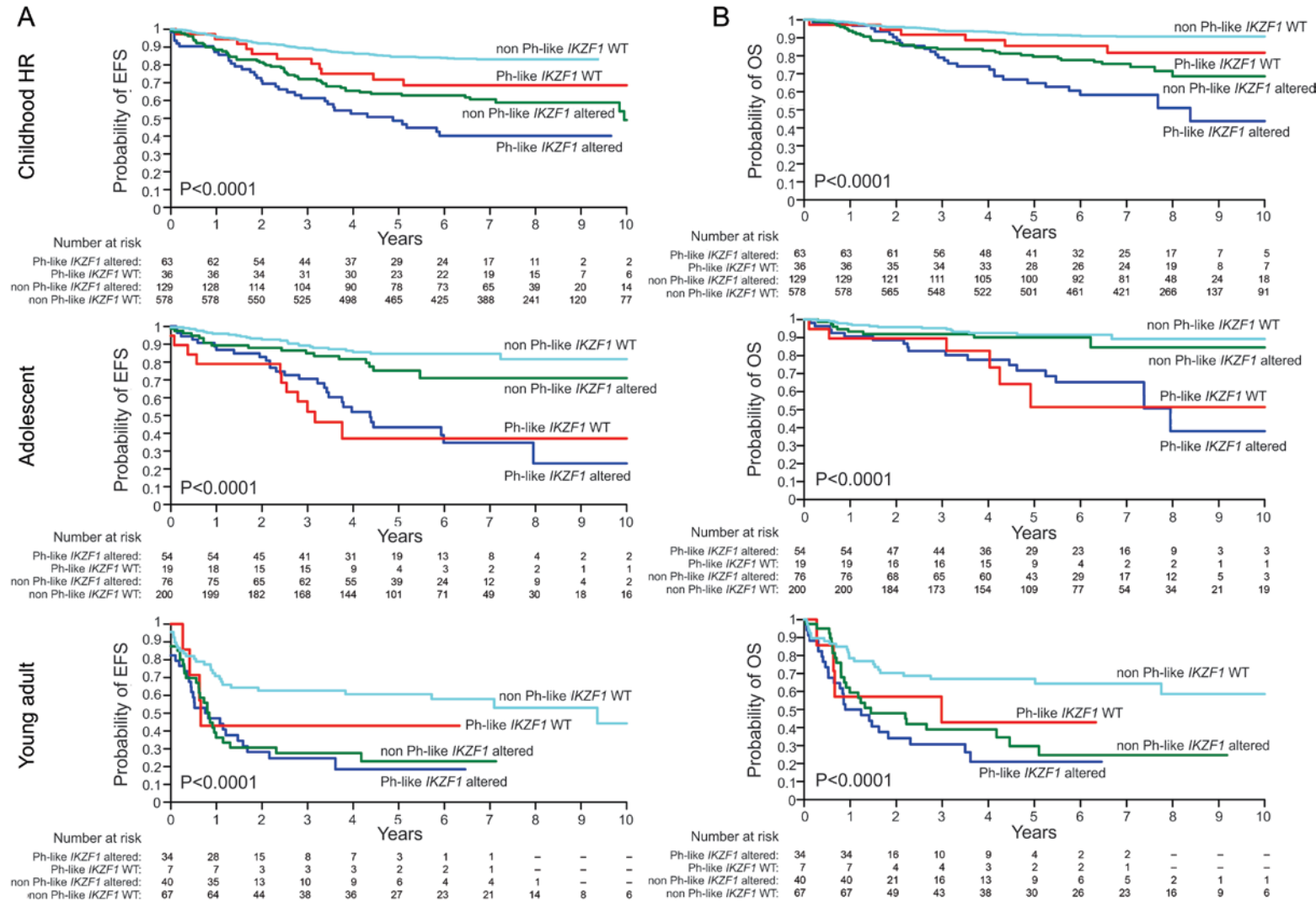


Figure S16. Experimental modeling of kinase fusions in Ph-like ALL

A) Expression of RCSD1-ABL1 (110 kDa), RCSD1-ABL2 (100 kDa), SSBP2-CSF1R (87 kDa), PAX5-JAK2 (59 kDa) and Ik6 (32 kDa) in murine interleukin-7 dependent *Arf*^{-/-} primary pre-B cells. B) Proliferation of Ba/F3 cells in the absence of cytokine and C) in the presence of dasatinib.

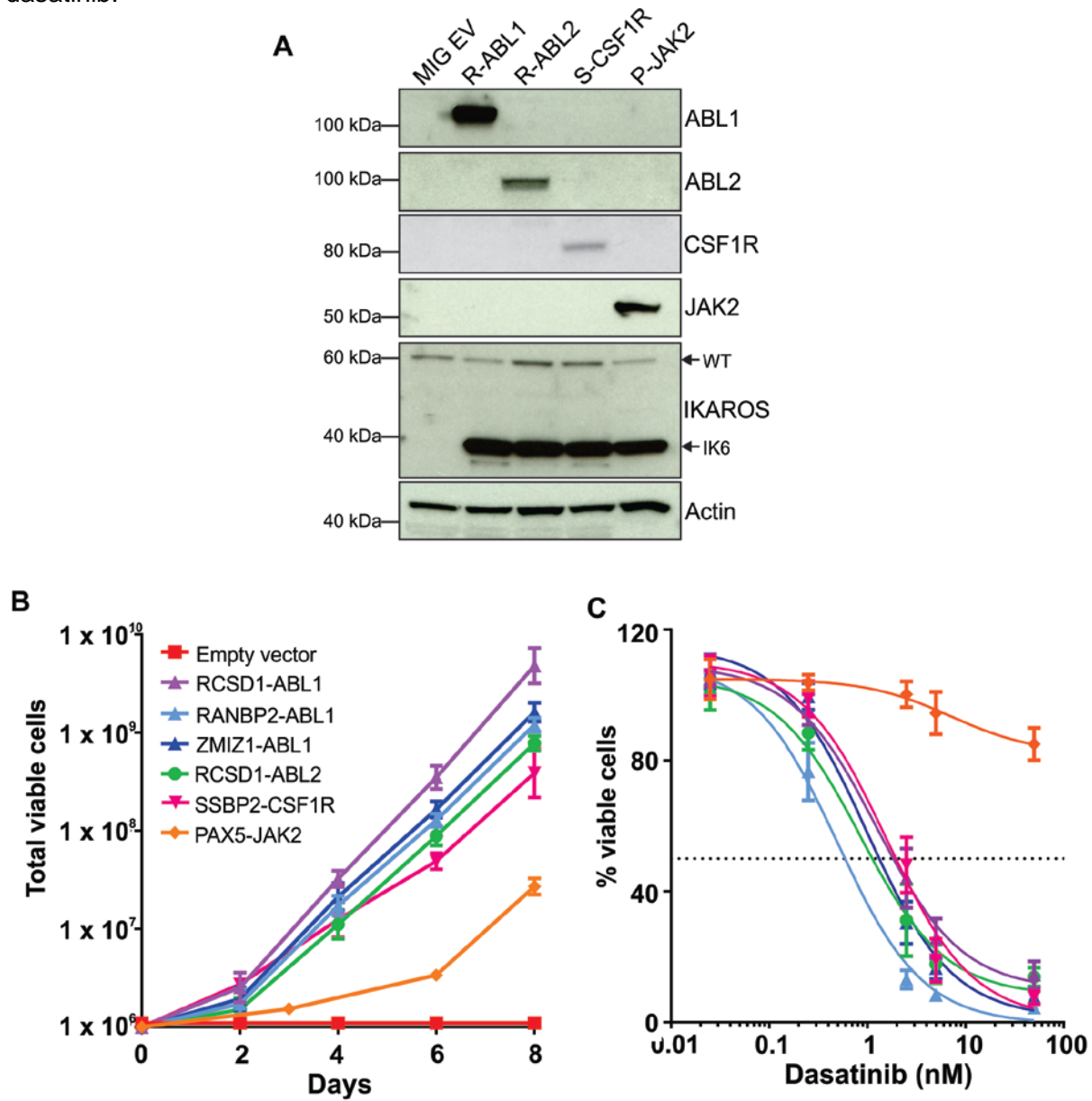


Figure S17. Treatment of Ph-like ALL xenografts with tyrosine kinase inhibitors

A) *Ex vivo* cytotoxicity assays of human leukemic cells harboring ATF7IP-JAK2 or IGH-EPOR. Both were sensitive to ruxolitinib, whilst imatinib had no effect on cell proliferation. B) *Ex vivo* cytotoxicity assay of human leukemic cells harboring ETV6-NTRK3 harvested from xenografted mice treated with crizotinib and imatinib. C) *In vivo* response of ETV6-ABL1 xenograft to dasatinib (20mg/kg/day 5 days per week) with a significant reduction in circulating human CD45+ leukemic cells and spleen weight. ***, $P < 0.001$.

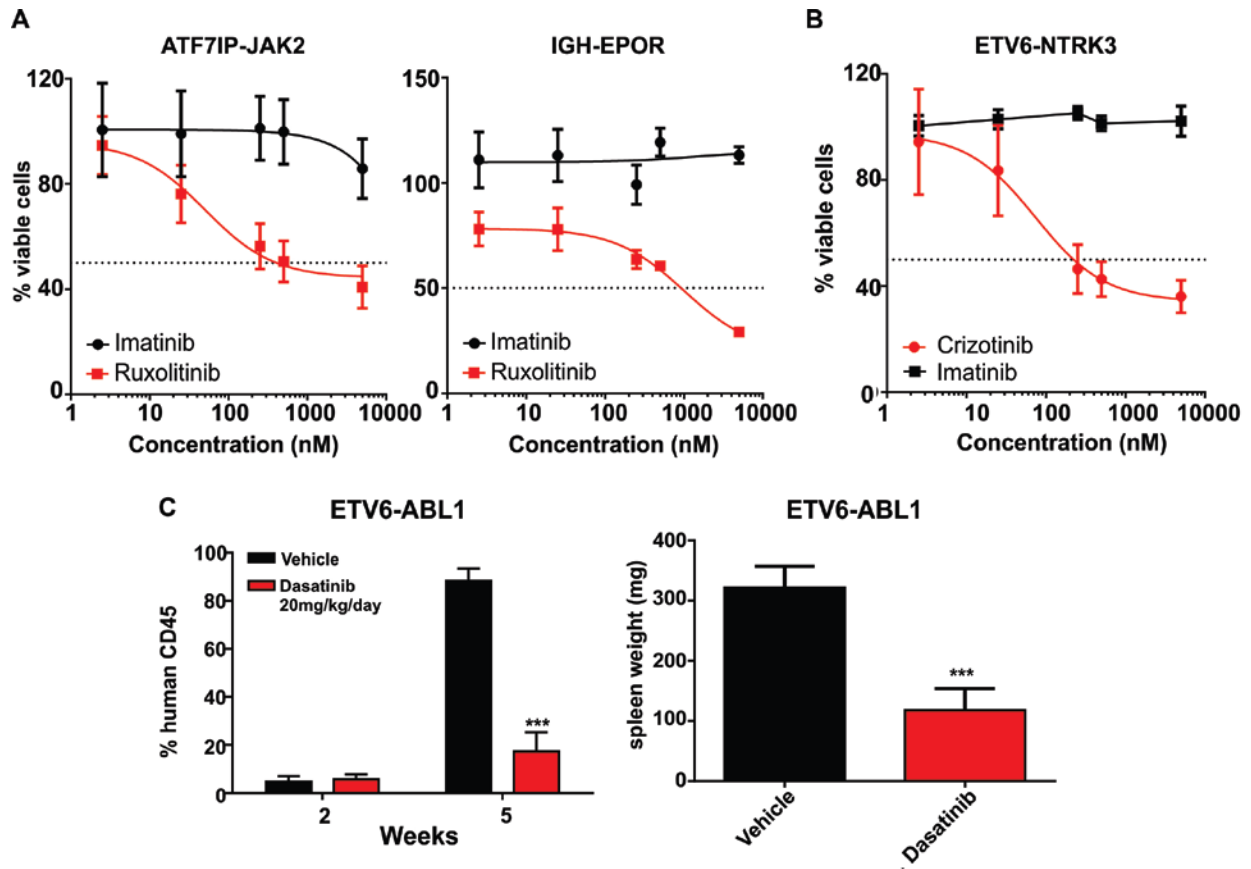


Figure S18. Flow chart for identification of Ph-like ALL cases and actionable kinase alterations

MLL rearranged, *TCF3-PBX1* and *ETV6-RUNX1* ALL cases do not exhibit a Ph-like gene expression profile. A minority of high hyperdiploid, low hypodiploid and near haploid ALL cases are Ph-like, hence inclusion of these entities in screening approaches. Immunophenotyping may also incorporate phosphoflow cytometry for signaling pathway activation (e.g. pSTAT5 and pCRKL) and response to kinase inhibition, but activation of these pathways is not specific for Ph-like ALL. The Ph-like gene expression signature may be identified with high sensitivity and specificity using gene expression profiling of a small number of genes (low density gene expression array)²⁶.

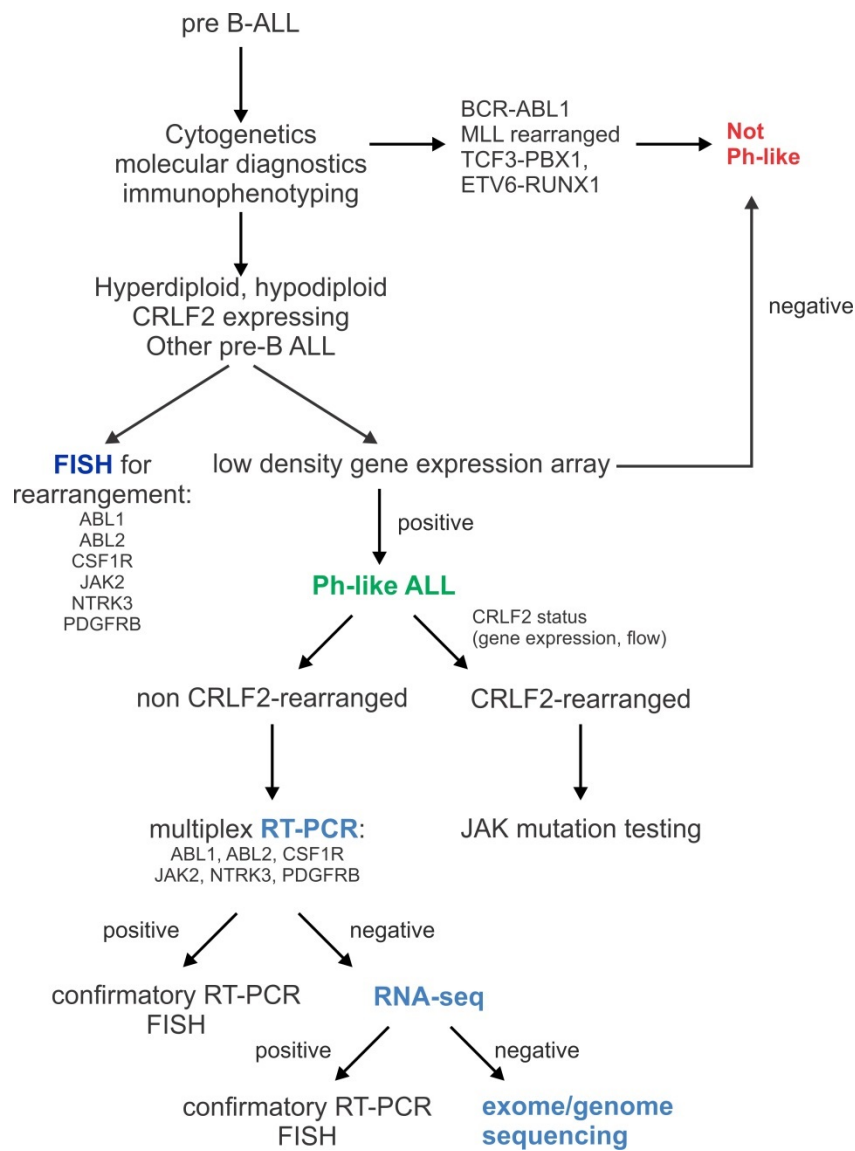
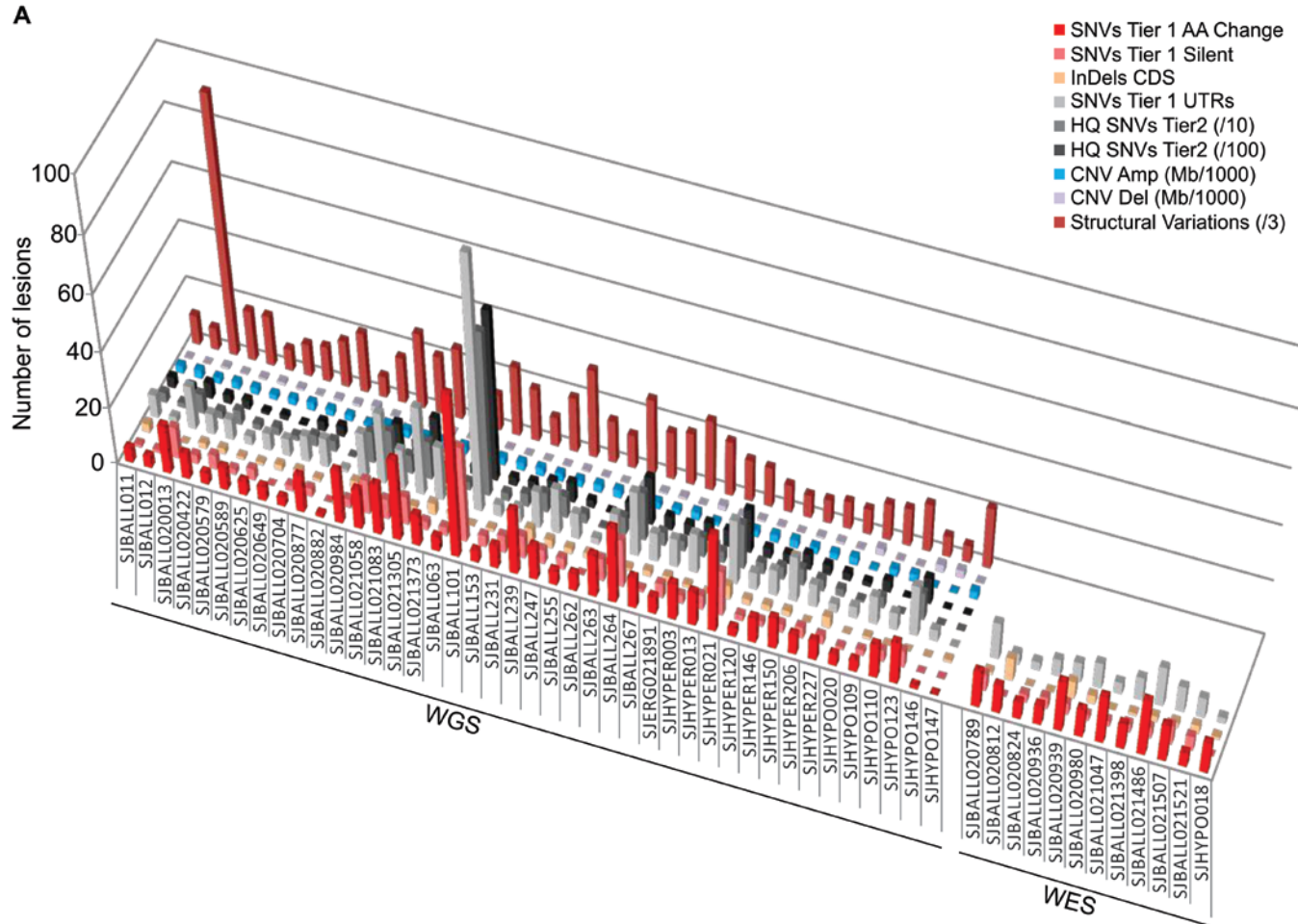


Figure S19. Sequence mutation analysis of Ph-like ALL.

A) Next generation sequenced cases are depicted from left to right. AA, amino acid; CDS, coding DNA sequence; HQ, high quality; UTR, untranslated region; tier 1, variants in coding regions, splice sites, UTRs and noncoding RNAs; tier 2, variants in conserved regions; WGS, whole genome sequencing; WES, whole exome sequencing; SNV, single nucleotide variation; CNV, copy number variation; Amp, amplification; Del, deletion; Mb, megabases.



B) Mutation frequencies from whole genome and whole exome data. Frequency per case of non-silent coding single nucleotide variants and insertion/deletions in 54 Ph-like cases analyzed by whole genome or whole exome sequencing. C) Recurrently mutated genes identified in 154 Ph-like cases by whole genome or whole exome sequencing, or mRNA-seq. Genes with non-silent coding variants (single nucleotide variants and insertion/deletions) found in ≥ 3 cases are shown.

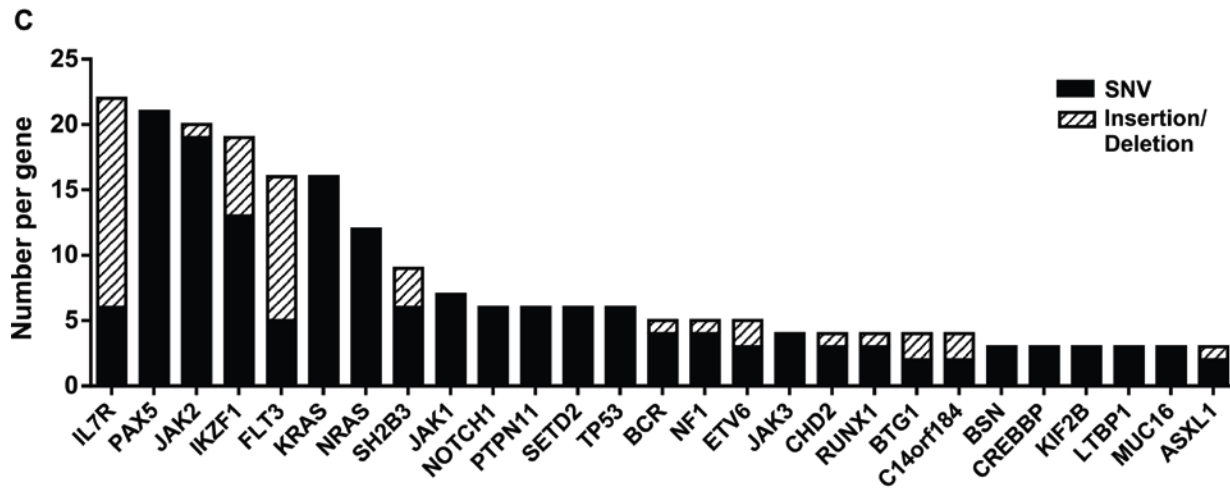
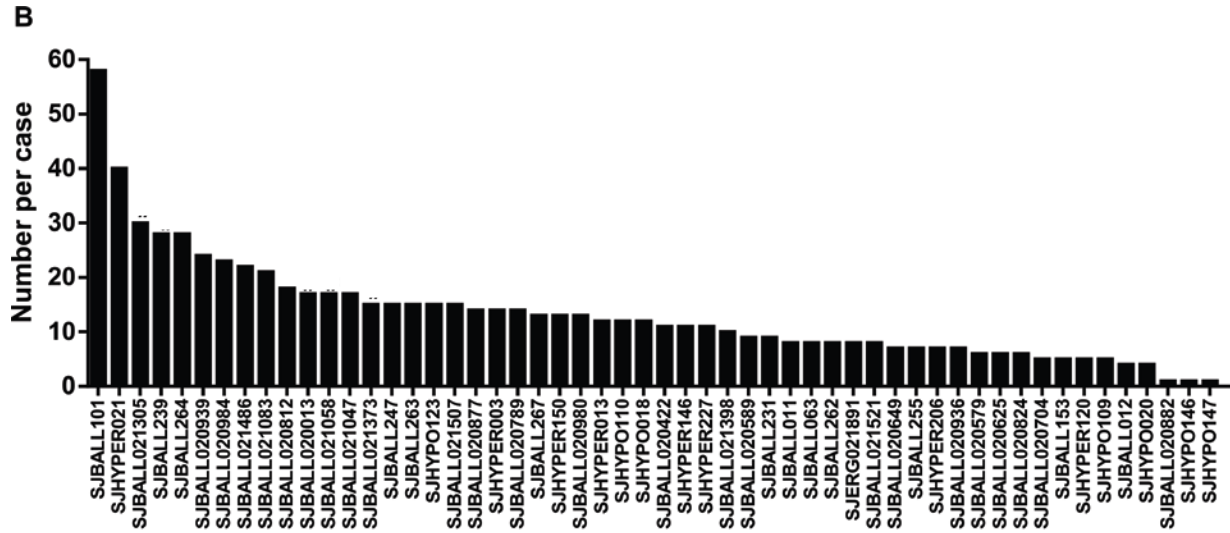
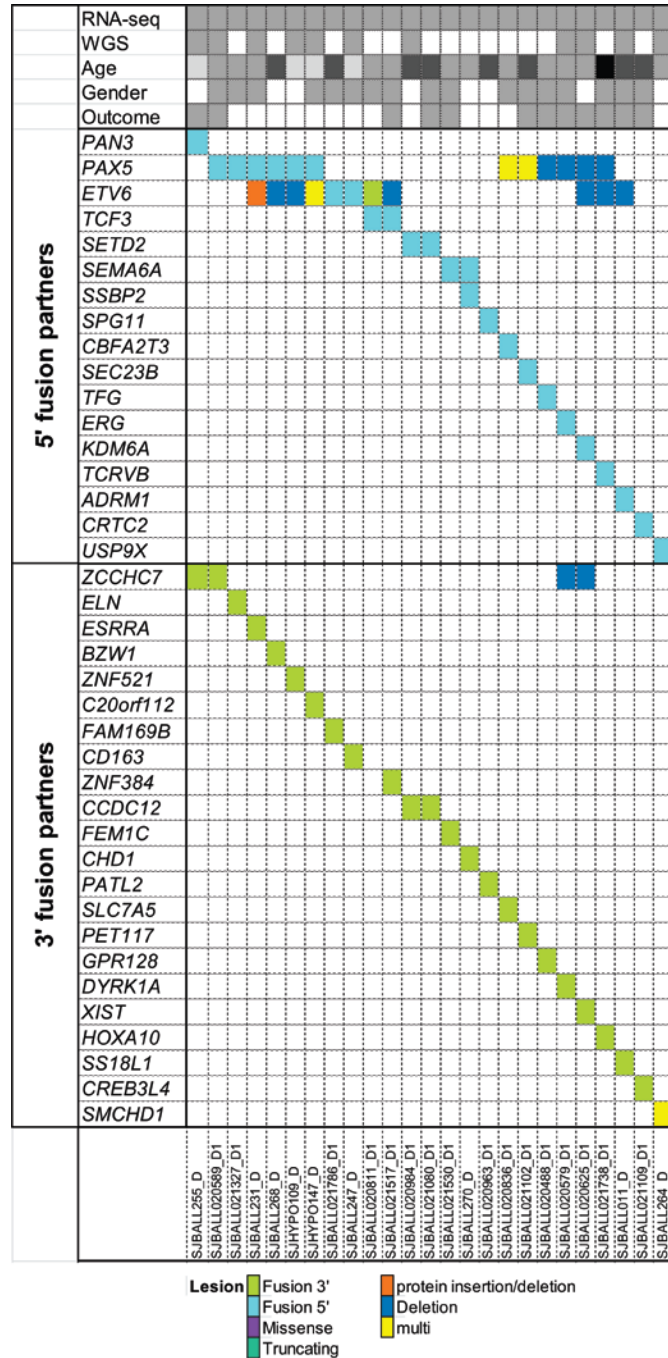


Figure S20. Non-kinase fusions

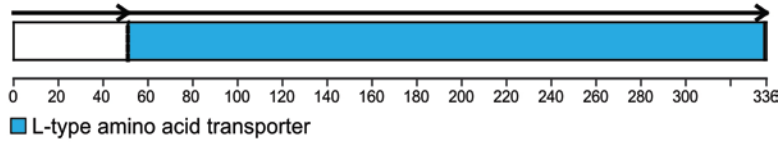
Heatmap (A) and protein domain plots (B) for non-kinase fusions identified in Ph-like ALL.

A

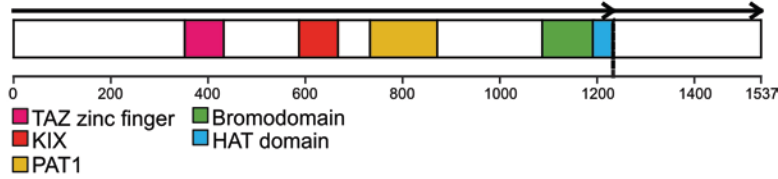


B

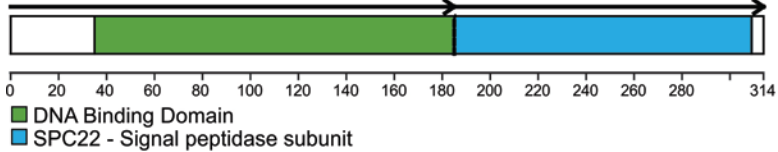
CBFA2T3-SLC7A5



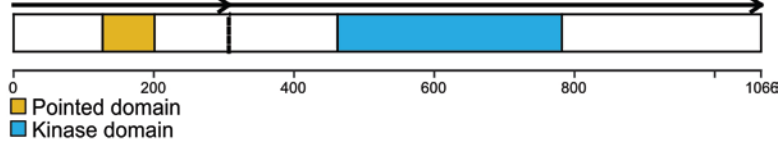
CREBBP-C7orf60



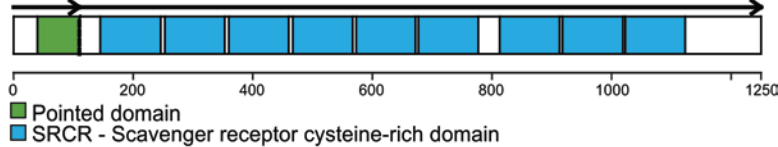
EBF1-SPCS3



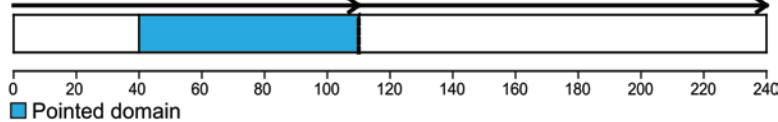
ERG-DYRK1A



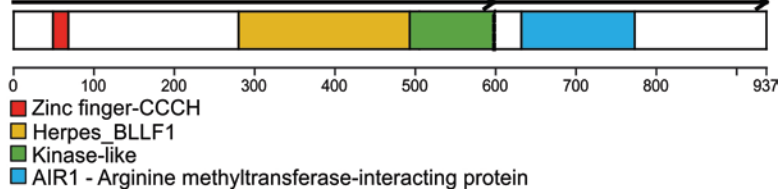
ETV6-CD163



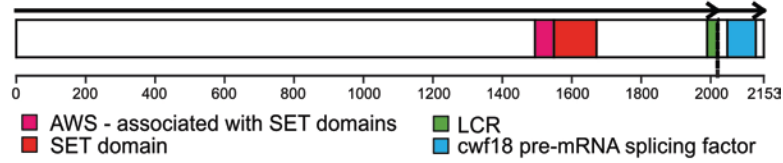
ETV6-FAM169B



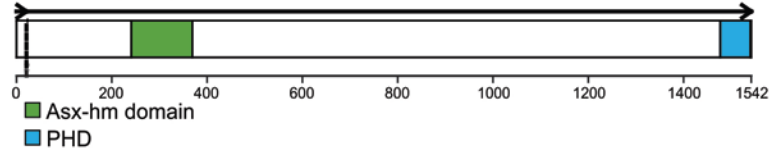
PAN3-ZCCHC7



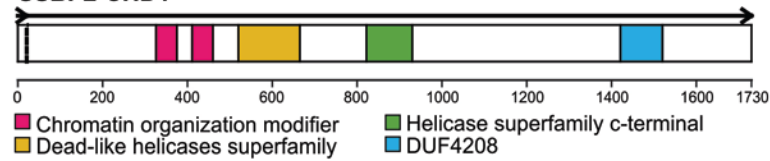
SETD2-CCDC12



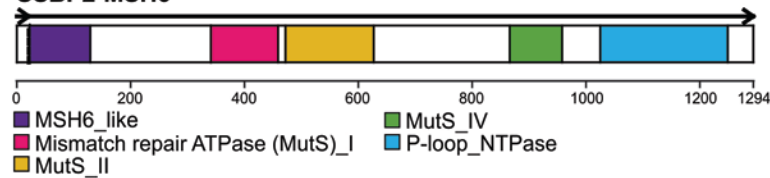
SSBP2-ASXL1



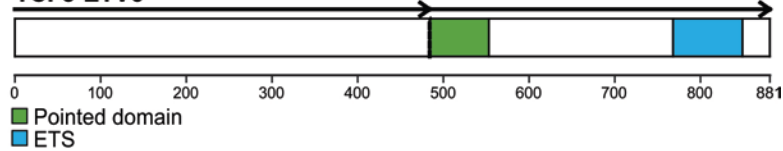
SSBP2-CHD1



SSBP2-MSH6



TCF3-ETV6



USP9X-SMCHD1

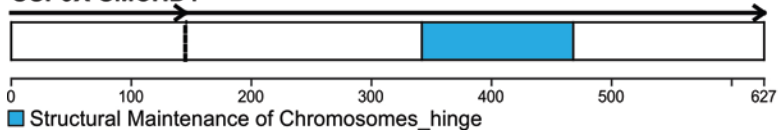
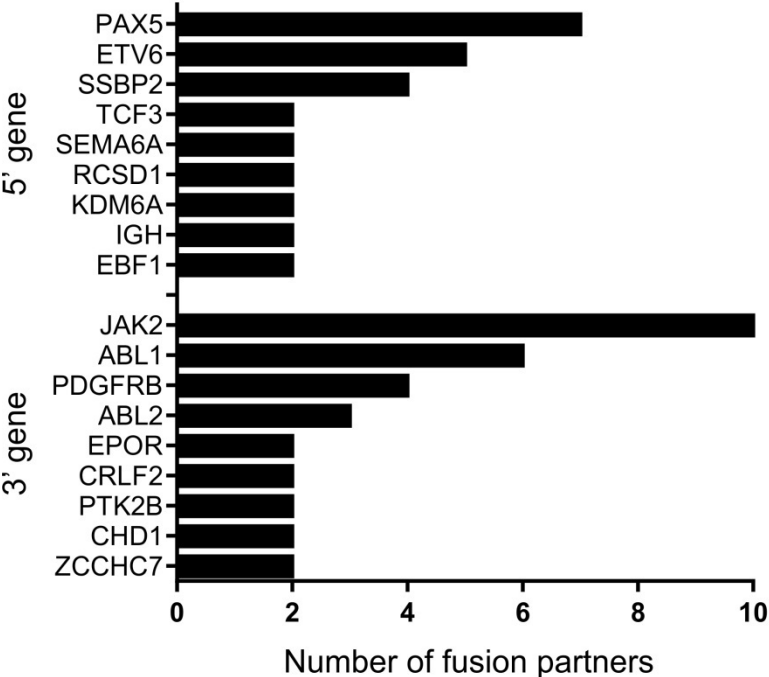


Figure S21. Genes involved in multiple rearrangements

Summary of different rearrangements involving 5' and 3' partner genes.



SUPPLEMENTARY TABLES

Table S1. Patient cohort

See Supplementary Appendix 1

Table S2. Clinical features and availability of genomic data

Comparison of clinical features - gender, age at diagnosis, white blood cell count (WBC) - of patients with and without gene expression profiling. Gender frequency was compared using Fisher's exact test. Age at diagnosis and WBC was compared using t-test.

Cohort	GEP	Male		Female		Total		P value
		N	%	N	%	N	%	
St Jude	Y	291	40.7%	261	36.5%	552	77.2%	0.53
	N	91	12.7%	72	10.1%	163	22.8%	
		382	53.4%	333	46.6%	715	100%	
COG	Y	591	58.2%	418	41.2%	1009	99.4%	0.41
	N	5	0.5%	1	0.1%	6	0.6%	
		596	58.7%	419	41.3%	1015	100%	
ECOG	Y	41	38.3%	33	30.8%	74	69.2%	0.54
	N	16	15%	17	15.9%	33	30.8%	
		57	53.3%	50	46.7%	107	100%	
MDACC	Y	21	38.2%	10	18.2%	31	56.4%	0.40
	N	13	23.6%	11	20.0%	24	43.6%	
		34	61.8%	21	38.2%	55	100%	
CALGB	Y	32	33%	13	13.4%	45	46.4%	0.39
	N	32	33%	20	20.6%	52	53.6%	
		64	66%	33	34%	97	100%	

Cohort	GEP	N	Age at diagnosis	P value
St Jude	Y	552	6.7	0.09
	N	163	7.3	
COG	Y	1009	11.4	0.05
	N	6	16.2	
ECOG	Y	75	29.3	0.28
	N	34	27.4	
MDACC	Y	31	26.7	0.99
	N	24	26.9	
CALGB	Y	45	25.5	0.84
	N	52	26.4	

Cohort	GEP	N	WBC (10 ⁹ /L)	P value
St Jude	Y	552	38.0	<0.001
	N	163	33.1	
COG	Y	1009	78.2	0.21
	N	6	79.0	
ECOG	Y	54	97.6	0.52
	N	10	61.7	
MDACC	Y	31	64.4	0.01
	N	24	27.4	
CALGB	Y	45	54.8	0.07
	N	52	52.1	

Table S3. B-ALL cases subjected to mRNA-sequencing

Subtype	Count
ERG	55
ETV6-RUNX1	54
Familial PAX5 pGly183Ser ALL	4
High hyperdiploid	1
Hypodiploid	8
iAMP21	8
Ph-like	136
Ph-positive ALL	27
T-lineage ALL	3

Table S4. Frequency of ALL subtypes in the study cohort

	Childhood SR		Childhood HR		Adolescent		Young adult		Total	
	N	%	N	%	N	%	N	%	N	%
BCR-ABL1	4	1.2	46	5.4	22	5.9	37	22.0	109	6.3
CRLF2 non-Ph-like	6	1.8	16	1.9	8	2.1	1	0.6	31	1.8
TCF3-PBX1	18	5.5	68	8.0	19	5.1	3	1.8	108	6.3
ERG	17	5.2	80	9.4	38	10.2	9	5.4	144	8.3
ETV6-RUNX1	101	30.6	72	8.4	14	3.7	3	1.8	190	11.0
Hyperdiploid	97	29.4	82	9.6	40	10.7	5	3.0	224	13.0
Hypodiploid	9	2.7	9	1.1	5	1.3	0	0.0	23	1.3
MLL	8	2.4	41	4.8	17	4.5	26	15.5	92	5.3
Other	37	11.2	331	38.8	134	35.8	38	22.6	540	31.3
Ph-like CRLF2	8	2.4	45	5.3	46	12.3	24	14.3	123	7.1
Ph-like non-CRLF2	25	7.6	63	7.4	31	8.3	22	13.1	141	8.2
Ph-like total	33	10	108	12.7	77	20.6	46	27.4	264	15.3
Total	330	100.0	853	100.0	374	100.0	168	100.0	1725	100.0

Table S5. Clinical characteristics and B-ALL subtype

Clinical characteristics (gender frequency and WBC) of BCR-ABL1, MLL-rearranged, Ph-like and Other B-ALL subtypes. WBC comparison by Kruskal-Wallis rank sum test. Gender comparison by Fisher's exact test between Ph-like and non Ph-like B-ALL (including BCR-ABL1, MLL-rearranged and all Other B-ALL).

Age	Subtype	N	WBC (x10 ⁹ /L)	P value
Childhood high-risk	BCR-ABL1	45	125.2	<0.001
	MLL-rearranged	41	189.6	
	Ph-like CRLF2r	44	151.7	
	Ph-like non CRLF2r	61	124.5	
	Other	656	76.4	
	TOTAL	847		
Adolescent	BCR-ABL1	22	117.6	<0.001
	MLL-rearranged	16	205.6	
	Ph-like CRLF2r	45	93.6	
	Ph-like non CRLF2r	31	49.2	
	Other	252	22.5	
	TOTAL	366		
Young Adult	BCR-ABL1	32	68.3	<0.001
	MLL-rearranged	22	150.4	
	Ph-like CRLF2r	21	90.9	
	Ph-like non CRLF2r	20	82.1	
	Other	51	17.3	
	TOTAL	146		

Age	Subtype	Male		Female		Total	P value
		N	%	N	%		
Childhood high-risk	BCR-ABL1	26	56.5%	20	43.5%	46	0.12
	MLL-rearranged	21	51.2%	20	48.8%	41	
	Ph-like	65	61.9%	40	38.1%	105	
	Other	352	53.7%	304	46.3%	656	
	TOTAL	464	54.7%	384	45.3%	848	
Adolescent	BCR-ABL1	12	54.5%	10	45.5%	22	0.07
	MLL-rearranged	8	47.1%	9	52.9%	17	
	Ph-like	56	72.7%	21	27.3%	77	
	Other	163	63.4%	94	36.6%	257	
	TOTAL	239	64.1%	134	35.9%	373	
Young Adult	BCR-ABL1	21	56.8%	16	43.2%	37	0.003
	MLL-rearranged	11	44%	14	56%	25	
	Ph-like	37	82.2%	8	17.8%	45	
	Other	37	62.7%	22	37.3%	59	
	TOTAL	106	63.9%	60	36.1%	166	

Table S6. Minimal residual disease (MRD) analyses

Children's Oncology Group childhood high-risk ALL, Day 28 MRD (P <0.001)

	Negative	Positive	
	N	N	Total
	%	%	
BCR-ABL1	13 52.00	12 48.00	25
Ph-like	50 58.14	36 41.86	86
MLL	15 78.95	4 21.05	19
all Other	446 89.02	55 10.98	501
Total	524	107	631

Children's Oncology Group adolescent ALL, Day 28 MRD (P <0.001)

	Negative	Positive	
	N	N	Total
	%	%	
BCR-ABL1	3 27.27	8 72.73	11
Ph-like	26 44.83	32 55.17	58
MLL	10 76.92	3 23.08	13
all Other	188 84.30	35 15.70	223
Total	227	78	305

Table S7. Multivariate analysis for childhood, adolescent and young adult B-ALL

Minimal residual disease (MRD) data were not available for the majority of adolescent and young adult patients, and were not included.

Childhood B-ALL including standard-risk and high-risk

Clinical features	Event-free survival			Overall survival		
	Hazard Ratios	95% CI	P value	Hazard Ratios	95% CI	P value
Age at diagnosis ≥ 10 yrs vs. <10 yrs	1.357	1.00-1.84	0.05	2.224	1.48-3.35	<0.001
MRD at end of induction Pos vs. Neg	3.583	2.67-4.82	<0.001	3.872	2.60-5.77	<0.001
WBC at diagnosis ≥100 vs. <100	1.947	1.43-2.65	<0.001	2.034	1.37-3.03	<0.001
Ph-like ALL vs ALL B-other	1.769	1.24-2.52	0.002	1.858	1.16-2.97	0.009

Adolescent and young adult B-ALL

Clinical features	Event-free survival			Overall survival		
	Hazard Ratios	95% CI	P value	Hazard Ratios	95% CI	P value
WBC at diagnosis ≥100 vs. <100	1.520	1.05-2.20	0.03	1.583	1.05-2.40	0.03
Ph-like ALL vs ALL B-other	3.455	2.37-5.03	<0.001	4.456	2.80-7.08	<0.001

Table S8. Sequencing coverage metrics

See Supplementary Appendix 1

Genomic Coverage: the average coverage of all non-ambiguous bases in GRCh37-lite.

Exon Coverage: the average coverage at all exonic bases (including all noncoding RNAs annotated in RefSeq).

% Genomic bases covered: the percentage of all non-ambiguous bases covered at least 10x.

% Exonic bases covered: the percentage of all bases in RefSeq annotated exons covered at least 10x.

% Coding bases covered: the percentage of all RefSeq protein coding bases covered at least 10x.

% SNP detection: concordance of genotype calls derived by WGS and those of Affymetrix SNP 6.0

Table S9. Summary of genetic alterations in Ph-like ALL

See Supplementary Appendix 1

Table S10. Gene expression profile of BCR-ABL1 and Ph-like ALL defined by mRNA-sequencing

See Supplementary Appendix 1

To define gene expression signatures, FPKM (fragments per kilobase of exon per million fragments mapped) was log₂ transformed and analyzed using linear models (Limma). Differentially expressed genes were selected using an FDR cutoff of 1%.

Table S11. Fusions detected by next-generation sequencing

See Supplementary Appendix 1

Description of all fusions identified in analyses of mRNA-seq, whole genome sequencing and whole exome sequencing data.

Table 12. Details of kinase fusions

See Supplementary Appendix 1

Table S13. Summary of 5' and 3' fusion partner genes with multiple rearrangements

Gene	Location in fusion transcript	Number of different fusion partners	Number of samples
ABL1	3'	6	13
ABL2	3'	3	7
CHD1	3'	2	3
CRLF2	3'	2	30
EPOR	3'	2	8
JAK2	3'	10	20
PDGFRB	3'	4	10
ZCCHC7	3'	2	2
EBF1	5'	2	7
ETV6	5'	5	8
IGH	5'	2	25
PAX5	5'	7	13
SSBP2	5'	8	12

Table S14. Subclonal mutation analysis in Ph-like ALL

Sample	Gene	AA_change	Mutant allele frequency (MAF)	Cases with subclonal MAF
SJBALL020704	IKZF1	G482fs	0.155556	
SJBALL020789	JAK2	I682F	0.148936	
SJBALL020789	JAK2	R683G	0.106383	
SJBALL020789	PAX5	P80R	0.64	
SJBALL020980	ETV6	I176V	0.333333	
SJBALL020980	ETV6	Y104fs	0.419355	
SJBALL020984	IL7R	L243_T244>RQGCP	0.196721	Yes
SJBALL020984	NRAS	G13D	0.311475	
SJBALL020984	SH2B3	L347fs	0.837838	
SJBALL020984	FLT3	ITD	0.2083	
SJBALL021047	PAX5	T75I	0.114286	
SJBALL021058	IKZF1	R502W	0.318182	Yes
SJBALL021058	SH2B3	S245_E3splice	0.972222	
SJBALL021058	FLT3	ITD	0.107	
SJBALL021083	JAK2	R683G	0.859649	
SJBALL021305	FLT3	PGGYEYDLinsK601	0.109091	Yes
SJBALL021305	JAK3	S789P	0.375	
SJBALL021373	IL7R	P240_S246>RAYC	0.14	Yes
SJBALL021373	PTPN11	N308S	0.25	
SJBALL021373	SH2B3	R398fs	0.5625	
SJBALL021398	KRAS	G13D	0.25	
SJBALL021486	IL7R	D239_T244>SFC	0.142857	Yes
SJBALL021486	IL7R	P240_T244>SCLI	0.142857	
SJBALL021486	JAK3	M511I	0.115385	
SJBALL021486	PAX5	G338R	0.467742	
SJBALL021507	IL7R	L243_T244>CAN	0.409091	
SJBALL021507	NRAS	G12S	0.194805	
SJBALL021507	PAX5	P80R	0.944444	
SJBALL063	PAX5	G183V	0.875	
SJBALL231	ETV6	R105>PR*	0.222222	Yes
SJBALL231	IL7R	V253G	0.204545	
SJBALL231	JAK1	F838L	0.2	
SJBALL231	PTPN11	A72V	0.173077	
SJBALL239	IL7R	I241_S246>TC	0.242424	
SJBALL239	IL7R	I241T	0.162162	
SJBALL239	IL7R	L243_S246>RVPGC	0.242424	
SJBALL247	KRAS	A146T	0.423077	
SJBALL262	IKZF1	L85_G94fs	0.342105	
SJBALL263	IL7R	L243_T244>RCPP	0.392857	

SJBALL264	KRAS	A18D	0.396825	
SJERG021891	KRAS	E63K	0.203704	
SJHYPER150	FLT3	A680V	0.225	
SJHYPER150	FLT3	GinsY597	0.08	
SJHYPER227	IKZF1	T40fs	0.403509	
SJHYPO018	NRAS	G12R	0.288462	
SJHYPO018	SH2B3	V402M	0.938462	
SJHYPO109	IL7R	V253G	0.47541	Yes
SJHYPO109	JAK1	A428P	0.227273	
SJHYPO110	NRAS	Q61K	0.23913	
SJHYPO146	NF1	T2133fs	0.051282	
SJHYPO146	PAX5	G25E	0.137931	
SJHYPO147	KRAS	G13D	0.617647	

Table S15. Outcome analyses for different subgroups in Ph-like ALL

Ph-like ALL subgroups	All ages combined			Childhood HR			AYA		
	N	5-year EFS	5-year OS	N	5-year EFS	5-year OS	N	5-year EFS	5-year OS
CRLF2r JAK mutant	67	38.8±7.0	55.5±7.0	26	46.2±9.8	61.3±9.5	38	28.2±9.8	50.0±10.7
CRLF2r JAK wild-type	52	56.5±7.9	64.3±7.8	19	73.0±10.1	84.2±8.6	28	35.4±11.6	40.3±11.8
ABL1-class	30	54.6±10.6	71.8±9.5	17	50.4±13.4	68.0±12.8	11	51.9±18.0	71.6±15.6
JAK2/EPOR	23	26.1±8.5	45.7±10.6	10	40.0±13.9	50.0±14.4	13	15.4±8.2	42.3±14.4
Other JAK-STAT	31	68.3±9.9	76.1±9.0	18	74.9±11.3	88.2±8.4	10	50.0±20.4	45.0±19.3
Ras pathway	14	85.7±11.5	100±0.0	5	80.0±17.9	100±0.0	5	80.0±25.3	100.0±0.0
Unknown	35	69.0±10.3	38.8±7.0	10	49.2±20.2	74.1±16.9	9	33.3±19.2	51.9±20.8

AYA, adolescent and young adult; EFS, event-free survival; OS, overall survival; HR, high-risk;

Table S16. Key genetic alterations in B-ALL

Frequency of deletions, mutations and/or rearrangements affecting key genes in ALL subgroups. B-cell pathway genes include *IKZF1*, *EBF1*, *PAX5*, *ETV6*, *TCF3*, *ERG*.

Group	IKZF1			EBF1		PAX5		B-cell pathway		CDKN2A/B	
	N	N	%	N	%	N	%	N	%	N	%
BCR-ABL1	109	77	70.6	12	11.1	38	34.9	86	78.9	41	37.6
CRLF2 non-Ph-like	31	14	45.2	2	6.5	16	51.6	23	74.2	18	58.1
E2A-PBX1	107	5	4.7	1	0.9	42	39.3	69	64.5	35	32.7
ERG	144	43	29.9	2	1.4	36	25	76	52.8	50	34.7
ETV6-RUNX1	190	4	2.1	12	6.3	57	30	94	49.5	58	30.5
Hyperdiploid	224	20	8.9	2	0.9	23	10.3	47	21.0	48	21.4
Hypodiploid	23	12	52.2	1	4.3	13	56.5	16	69.6	13	56.5
MLL	92	10	10.9	0	0	7	7.6	20	21.7	16	17.4
Other	540	95	17.6	17	3.1	211	39.1	304	56.3	268	49.6
Ph-like CRLF2	123	96	78.0	36	29.3	53	43.1	109	88.6	64	52.0
Ph-like non-CRLF2	141	70	49.6	19	13.5	44	31.2	98	69.5	50	35.5
Total	1725	446	25.9	104	6.0	540	31.3	942	54.6	661	38.3

Table S17. B-ALL cases tested prospectively for Ph-like status

Summary of B-ALL cases referred for high-risk clinical features (refractory to treatment or high white blood cell count), or suggestion of a rearrangement involving a kinase gene on cytogenetic and/or FISH analysis. Ph-like status was determined using a low density gene expression array card and fusion status was determined using either RT-PCR or mRNA-seq analysis. Details of cases treated with tyrosine kinase inhibitors are provided in the Supplementary Results.

Sample ID	Age (Years)	WBC X10 ⁹ /L	Cytogenetics	FISH	Ph-like	Kinase alteration	Comments	Tyrosine kinase inhibitor
PAUXZX	5.0	322	46,XX,t(9;12)(q34;p13)[18]/46,XX[2]	<i>ABL 1</i> -rearranged	Yes	<i>ETV6-ABL 1</i>		
ALL002	82	183	46,XY, del (6) (q13p25-27), +11 [3]/48, sl, +6 [8]/45-46	<i>ABL 1</i> -rearranged	Yes	<i>ETV6-ABL 1</i>		Dasatinib
PAWDPK	9	27	47,XY,+X,t(3;9)(p13;q34)[19]/46,XY[1]	<i>ABL 1</i> -rearranged	Yes	<i>FOXP1-ABL 1</i>		Dasatinib
PAVZZE	12	88	46,XY	Additional <i>ABL 1</i>	N/A	<i>NUP214-ABL 1</i>	Day 29 MRD 12.4%	Dasatinib
PAVVIE	12.1	567	46,XX,der(6)t(6;9)(p23;q34),der(9)del(9)(p13p22)t(6;9),-20,+mar[13]/48,sl,+8,+10[2]/46,XX[5]	<i>ABL 1</i> -rearranged	Yes	<i>NUP153-ABL 1</i>	Novel fusion	
PAWALS	12.6	905	46,XY,t(2;9)(q11.2;q34)[20]	<i>ABL 1</i> -rearranged	Yes	<i>RANBP2-ABL 1</i>		Imatinib
PAVVKH	2.7	86	46,XX,t(2;9)(q11.2;q34)[4]/47,idem,+der(2)t(2;9)(q11.2;q34)[3]/46,XX[13]	<i>ABL 1</i> -rearranged	Yes	<i>RANBP2-ABL 1</i>		
PAVKDX	6.9	108	46,XY,t(1;9)(q23;q34)[6]/46,XY[14]	<i>ABL 1</i> -rearranged	Yes	<i>RCSD1-ABL 1</i>	Day 29 MRD 16.4%	Imatinib
PAVYCL	11.6	349	46,XX	<i>ABL 1</i> -rearranged	Yes	<i>ZMIZ1-ABL 1</i>	Day 29 MRD 5.4%	Dasatinib
PAVRNM	2.2	12	47,XY,der(3)(10qter->10q22.3::3q21->3p25::3q21>3qter),der(9)t(3;9)(p25;q34.3),der(10)t(9;10)(q34.3;q22.3),+14[14].ish der(10)t(9;10)(ASS-,ABL1+)/46,XY[11]	<i>ABL 1</i> -rearranged	Yes	<i>ZMIZ1-ABL 1</i>		
PAVXFI	2.6	148	45,XX,der(8)r(8;?)(p23q?22;?)[cp3]/43,sl,psudic(12;7)(p11.2;p22),der(9;22)(q10;q10),-13[12]/57,XX,+X,+2,+3,+6,+7,+8,i(8)(q10),+19,+21,+22,del(22)(q11.2x2),+mar1,+mar2[cp4]/46,XX[9]	<i>ABL 1</i> -rearranged	Yes	<i>ZMIZ1-ABL 1</i>		
PAVUCR	1.8	5.3	46,XY,t(9;10)(q34;q22)[5]/46,XY[28]	<i>ABL 1</i> -rearranged	No	<i>ZMIZ1-ABL 1</i>		

Sample ID	Age (Years)	WBC X10 ⁹ /L	Cytogenetics	FISH	Ph-like	Kinase alteration	Comments	Tyrosine kinase inhibitor
PAVMLC	5.6	58	47,XXYc[22]	<i>ABL2</i> -rearranged	Yes	<i>RCS1-ABL2</i>	Day 29 MRD 1.2%	Imatinib
PAVWWX	6.4	170	46,XY,t(1;7)(q21;q32)[7]/46,XY[13]	N/A	Yes	<i>ZC3HAV1-ABL2</i>	Day 29 MRD 36%	Dasatinib
PAUXVE	10.4	243	46,XX,t(1;7)(q25;q34)[2]/46,XX[5]	<i>ABL2</i> -rearranged	Yes	<i>ZC3HAV1-ABL2</i>		
PAVYXD	7.6	35	N/A	<i>CRLF2</i> -rearranged	Yes	<i>IGH-CRLF2</i>		
PAVZKV	16.3	7.6	46,XX,del(20)(q11.2q13.3)[11]/46,XX[9]	<i>CRLF2</i> -rearranged	Yes	<i>IGH-CRLF2</i>	High <i>CRLF2</i> expression by flow	
PAWBYB	19.5	16	46,XX,t(9;17)(p21;q25)[11]/46,XX[9]	N/A	N/A	<i>P2RY8-CRLF2</i>	High <i>CRLF2</i> expression by flow	
PAVUJE	15.0	246	46,XY[20]	Normal	Yes	<i>P2RY8-CRLF2</i>	Day 29 MRD 20%	
PAVUPA	2.6	7	46,XX,t(9;12)(p24;p13)[11]/46,XX[1]	N/A	Yes	<i>ETV6-JAK2</i>		
PAVZDC	5.3	88	46,XX,add(5)(q33),add(9)(p21)[13]/46,XX[11]	<i>ABL1</i> Normal	Yes	<i>PAX5-JAK2</i>		
ALL021	14	160	t(5;9)(q12;p1?3)	<i>JAK2</i> -rearranged	Yes	<i>SSBP2-JAK2</i>	Day 29 MRD 5.5%	Ruxolitinib
PAVMJD	6	244	46,XY	<i>PDGFRB</i> -rearranged	Yes	<i>EBF1-PDGFRB</i>	Day 29 42% blasts, induction failure	Imatinib
PAVZXA	14.4	42	47,XY,der(1)t(1;6)(q12;p21.3),+5,der(6)del(6)(p11.2p21.3)t(1;6)(q12;p21.3)[13]/46,XY[7]	N/A	Yes	<i>EBF1-PDGFRB</i>	Day 29 MRD 25.0%, induction failure	Dasatinib
ALL024	7	600	46,XY	Additional <i>PDGFRB</i>	N/A	<i>EBF1-PDGFRB</i>	Day 29 96% blasts, induction failure	Imatinib and dasatinib
PAVRSD	19.8	55	N/A	N/A	Yes	<i>EBF1-PDGFRB</i>	Induction failure, alive in remission post transplant	
PAVTGA	6.0	42	53,XY,+X,+4,+6,+14,der(15)t(5;15)(q32;q26),+17,+18,+21[7]/54,sl,+21[4]/46,XY[9]	<i>PDGFRB</i> -rearranged	No	<i>TNIP1-PDGFRB</i>	Day 29 MRD 0.14%	
PAVZDM	14.6	114	46,XY,t(5;14)(q31;q32)[4]/47,idem,+X[2]/46,XY[20]	<i>IGH-R</i> with <i>IL3</i>	Yes	Negative	62% eosinophils	
PAWAJT	4.4	59	46,XX,del(9)(p22p24),der(9)t(9*;9)(p24;q34),der(19)t(1;19)(q23;p13.3)[cp3]/46,XX[20]	Variant <i>ABL1</i> rearranged	Border	N/A		

Sample ID	Age (Years)	WBC X10 ⁹ /L	Cytogenetics	FISH	Ph-like	Kinase alteration	Comments	Tyrosine kinase inhibitor
PAVWVN	4.5	27	N/A	N/A	No	No	Day 8 PB MRD 0.31%; Day 29 BM MRD 0.15%; end consolidation MRD 0.084%	
PAVZCJ	13.5	17	46,XX,add(2)(p13),del(5)(q31q33),add(9)(p13)[6]/46,XX[14]	PDGFRB normal	N/A	No	Referred due to deletion of chromosome 5	
PAWCBU	13.2	7	46,XY,del(1)(q31),add(5)(q33),del(6)(q13q22),+8,del(8)(q13q22),dic(9;17)p11;p11.1,-13,20,+21,+mar[9]/46,XY[11]	PDGFRB normal	No	Negative	Referred due to 5q alteration	

Table S18. Primer sequences for fusion verification, cloning and genomic PCR

See Supplementary Appendix 1

Table S19. Probes used for fluorescence *in situ* hybridization

Fusion Gene	Gene	Clone ID
<i>BCR-JAK2</i>	<i>BCR</i>	RP11-165G5
	<i>JAK2</i>	RP11-356C24
	<i>JAK2</i>	RP11-729C13
<i>ETV6-JAK2</i>	<i>ETV6</i>	RP11-94N22
<i>PAX5-JAK2</i>	<i>PAX5</i>	RP11-652D9
<i>PPFIBP1-JAK2</i>	<i>PPFIBP1</i>	RP11-798N23
<i>RCSD1-ABL2</i>	<i>RCSD1</i>	RP11-784D17
	<i>ABL2</i>	RP11-1087A22
	<i>ABL2</i>	RP11-170H10
<i>TPR-JAK2</i>	<i>TPR</i>	RP11-367J1
<i>SSBP2-JAK2</i>	<i>SSBP2</i>	RP11-452C10
<i>IGH-EPOR</i>	<i>IGH</i>	RP11-150I16
	<i>IGH</i>	RP11-18C13
	<i>IGH</i>	RP11-953L20
	<i>IGH</i>	RP5-998D24
	<i>EPOR</i>	RP11-1114G9
	<i>EPOR</i>	RP11-478I13
	<i>EPOR</i>	RP11-109L17

Table S20. Summary of sequence mutations in Ph-like ALL

See excel workbook: "Table_S20_SNV_indel.xlsx"

Table S21. Summary of non-kinase fusions and association with kinase alterations.

PCGP ID	Kinase alteration	Ras pathway	Other fusion
SJBALL021786	FLT3 Y591 and T582 and SH2B3 L224fs		ETV6-FAM169B
SJBALL021794	Not by RNA-seq		CREBBP-ATG16L1
SJBALL021738	Not by RNA-seq		TCRVB-HOXA10
SJBALL021413	IL7R LT243-244>RCP		SS18L1-RBM38
SJBALL021327	JAK1 S646F	NRAS G12D	PAX5-ELN
SJBALL020013	P2RY8-CRLF2, Homozygous SH2B3 deletion		IQGAP2-TSLP
SJBALL020488			TFG-GPR128
SJBALL264		KRAS A18D	USP9X-SMCHD1
SJBALL020811			TCF3-ETV6
SJBALL020836			CBFA2T3-SLC7A5
SJBALL020579	IGH-EPOR		ERG-DYRK1A
SJBALL020625	ZC3HAV1-ABL2		KDM6A-XIST
SJBALL020852			SYNCRIP-PNRC1
SJBALL020853	P2RY8-CRLF2		SS18L1-RBM38
SJBALL020984	FLT3 V581	NRAS G13D	SETD2-CCDC12
SJBALL021080			SSBP2-MSH6 and SETD2-CCDC12
SJHYPO109	IL7R V253G and JAK1 mut		PAX5-ZNF521
SJBALL247		KRAS A146T	ETV6-CD163
SJBALL255			PAN3-ZCCHC7
SJHYPO147		KRAS G13D	PAX5-C20orf112
SJBALL231	IL7R and JAK1 mut		PAX5-ESRRA

SUPPLEMENTARY REFERENCES

1. Pui CH, Campana D, Pei D, et al. Treating childhood acute lymphoblastic leukemia without cranial irradiation. *N Engl J Med* 2009;360:2730-41.
2. Bowman WP, Larsen EL, Devidas M, et al. Augmented therapy improves outcome for pediatric high risk acute lymphocytic leukemia: Results of Children's Oncology Group trial P9906. *Pediatr Blood Cancer* 2011;57:569-77.
3. Goldstone AH, Richards SM, Lazarus HM, et al. In adults with standard-risk acute lymphoblastic leukemia, the greatest benefit is achieved from a matched sibling allogeneic transplantation in first complete remission, and an autologous transplantation is less effective than conventional consolidation/maintenance chemotherapy in all patients: final results of the International ALL Trial (MRC UKALL XII/ECOG E2993). *Blood* 2008;111:1827-33.
4. Kantarjian H, Thomas D, O'Brien S, et al. Long-term follow-up results of hyperfractionated cyclophosphamide, vincristine, doxorubicin, and dexamethasone (Hyper-CVAD), a dose-intensive regimen, in adult acute lymphocytic leukemia. *Cancer* 2004;101:2788-801.
5. Ravandi F, O'Brien S, Thomas D, et al. First report of phase 2 study of dasatinib with hyper-CVAD for the frontline treatment of patients with Philadelphia chromosome-positive (Ph+) acute lymphoblastic leukemia. *Blood* 2010;116:2070-7.
6. Thomas DA, Faderl S, Cortes J, et al. Treatment of Philadelphia chromosome-positive acute lymphocytic leukemia with hyper-CVAD and imatinib mesylate. *Blood* 2004;103:4396-407.
7. Thomas DA, O'Brien S, Faderl S, et al. Chemoimmunotherapy with a modified hyper-CVAD and rituximab regimen improves outcome in de novo Philadelphia chromosome-negative precursor B-lineage acute lymphoblastic leukemia. *J Clin Oncol* 2010;28:3880-9.

8. Stock W, Johnson JL, Stone RM, et al. Dose intensification of daunorubicin and cytarabine during treatment of adult acute lymphoblastic leukemia: results of Cancer and Leukemia Group B Study 19802. *Cancer* 2013;119:90-8.
9. Mullighan CG, Su X, Zhang J, et al. Deletion of IKZF1 and prognosis in acute lymphoblastic leukemia. *N Engl J Med* 2009;360:470-80.
10. Zhang J, Ding L, Holmfeldt L, et al. The genetic basis of early T-cell precursor acute lymphoblastic leukaemia. *Nature* 2012;481:157-63.
11. Roberts KG, Morin RD, Zhang J, et al. Genetic alterations activating kinase and cytokine receptor signaling in high-risk acute lymphoblastic leukemia. *Cancer Cell* 2012;22:153-66.
12. Tibshirani R, Hastie T, Narasimhan B, Chu G. Diagnosis of multiple cancer types by shrunk centroids of gene expression. *Proc Natl Acad Sci U S A* 2002;99:6567-72.
13. Harvey RC, Mullighan CG, Wang X, et al. Identification of novel cluster groups in pediatric high-risk B-precursor acute lymphoblastic leukemia with gene expression profiling: correlation with genome-wide DNA copy number alterations, clinical characteristics, and outcome. *Blood* 2010;116:4874-84.
14. Mullighan CG, Goorha S, Radtke I, et al. Genome-wide analysis of genetic alterations in acute lymphoblastic leukaemia. *Nature* 2007;446:758-64.
15. Venkatraman ES, Olshen AB. A faster circular binary segmentation algorithm for the analysis of array CGH data. *Bioinformatics* 2007;23:657-63.
16. Pounds S, Cheng C, Mullighan C, Raimondi SC, Shurtleff S, Downing JR. Reference alignment of SNP microarray signals for copy number analysis of tumors. *Bioinformatics* 2009;25:315-21.
17. Holmfeldt L, Wei L, Diaz-Flores E, et al. The genomic landscape of hypodiploid acute lymphoblastic leukemia. *Nat Genet* 2013;45:242-52.
18. Trapnell C, Hendrickson DG, Sauvageau M, Goff L, Rinn JL, Pachter L. Differential analysis of gene regulation at transcript resolution with RNA-seq. *Nat Biotechnol* 2013;31:46-53.

19. Mullighan CG, Collins-Underwood JR, Phillips LA, et al. Rearrangement of CRLF2 in B-progenitor- and Down syndrome-associated acute lymphoblastic leukemia. *Nat Genet* 2009;41:1243-6.
20. Harvey RC, Mullighan CG, Chen IM, et al. Rearrangement of CRLF2 is associated with mutation of JAK kinases, alteration of IKZF1, Hispanic/Latino ethnicity, and a poor outcome in pediatric B-progenitor acute lymphoblastic leukemia. *Blood* 2010;115:5312-21.
21. Williams RT, den Besten W, Sherr CJ. Cytokine-dependent imatinib resistance in mouse BCR-ABL+, Arf-null lymphoblastic leukemia. *Genes Dev* 2007;21:2283-7.
22. Williams RT, Roussel MF, Sherr CJ. Arf gene loss enhances oncogenicity and limits imatinib response in mouse models of Bcr-Abl-induced acute lymphoblastic leukemia. *Proc Natl Acad Sci U S A* 2006;103:6688-93.
23. Mullighan CG, Zhang J, Harvey RC, et al. JAK mutations in high-risk childhood acute lymphoblastic leukemia. *Proc Natl Acad Sci U S A* 2009;106:9414-8.
24. Shultz LD, Lyons BL, Burzenski LM, et al. Human lymphoid and myeloid cell development in NOD/LtSz-scid IL2R gamma null mice engrafted with mobilized human hemopoietic stem cells. *J Immunol* 2005;174:6477-89.
25. Schultz KR, Bowman WP, Aledo A, et al. Improved early event-free survival with imatinib in Philadelphia chromosome-positive acute lymphoblastic leukemia: a children's oncology group study. *J Clin Oncol* 2009;27:5175-81.
26. Harvey RC, Kang H, Roberts KG, et al. Development and Validation Of a Highly Sensitive and Specific Gene Expression Classifier To Prospectively Screen and Identify B-Precursor Acute Lymphoblastic Leukemia (ALL) Patients With a Philadelphia Chromosome-Like ("Ph-like" or "BCR-ABL1-Like") Signature For Therapeutic Targeting and Clinical Intervention. *Blood* 2013;122:826.